



This Project has received funding from European Commission by means of Horizon 2020, The EU Framework Programme for Research and Innovation, under Grant Agreement no. 700174

WWW.RESCCUE.EU

#resccueEU

RESCCUE

RESILIENCE TO COPE WITH CLIMATE CHANGE IN URBAN AREAS.

Summary report: Climate change scenarios

R. Monjo¹, C. Paradinas¹, J. Pórtoles¹, E. Gaitán¹, D. Redolat¹, C. Prado-López¹, M. Velasco², B. Russo², A. Jennings-Howe³, L. M. David⁴, A. Gabas⁵, R. Matos⁴, J. R. Stevens³, L. Pouget⁶, S. Vela⁶, J. Ribalaygua¹, I.C. Silva⁷, J. Telhado⁸, L. Coelho⁸, M. Morais⁸, S. Baltazar⁸

¹Climate Research Foundation (FIC);

²Aquatec; ³Bristol City Council; ⁴Laboratório Nacional de Engenharia Civil (LNEC);

⁵Barcelona City Council; ⁶Cetaqua; ⁷EDPDistribuição; ⁸Câmara Municipal de Lisboa (CML)

10 January 2019



Abstract	3
1. Introduction	4
1.1. Context	4
1.2. Report objectives and challenges	4
1.3. Structure of the report	5
2. Study area and data collection	6
2.1. Study area	6
2.2. Climate hazards identification	8
2.3. Observed variables	10
2.4. Climate models	10
3. Methodology	11
3.1. Climate simulation	11
3.1.1. General scheme	11
3.1.2. Statistical downscaling methods	12
3.2. Extreme events	17
3.2.1. Common criteria	17
3.2.2. Application to each time scale	19
3.3. Uncertainty analysis	21
4. Results of verification and validation	23
4.1. Mean climate	23
4.1.1. Verification	23
4.1.2. Climate models validation	23
4.1.3. Decadal dynamical method validation	24
4.2. Extreme events	25
4.2.1. Validation for the climate scale	25
4.2.2. Validation of decadal simulations	26
4.2.3. Seasonal validation	28
5. Mean climate and decadal scenarios	29
5.1. Barcelona	29
5.2. Lisbon	30
5.3. Bristol	30
6. Extreme events scenarios	32
6.1. Barcelona	33
6.2. Lisbon	36
6.3. Bristol	39
7. Conclusions	42
References	43

Abstract

RESCCUE project was devised to analyse future urban impacts due to climate change so as to improve resilience of three target cities: Barcelona, Bristol and Lisbon. To achieve that, future climate projections and changes in extreme events were obtained at a local scale. Several past studies were analysed to identify all the climate variables and extreme events that could affect urban areas, e.g. heavy rainfall, heat waves and storm surge. All available meteorological observations in the considered areas were collected and filtered through several tests (general consistency, outliers and inhomogeneities) in order to handle datasets long enough and of good quality. As a way to obtain the best input possible, every valid station was extended in time by downscaling process with ERA-Interim.

Future climate projections were obtained for ten different global climate models considering two of the main Representative Concentration Pathways (RCP4.5 and RCP8.5) established in the last IPCC report. These models were downscaled through a sophisticated statistical methods (analogous stratification and transfer functions among others) to project local climate according to the identified climate drivers: temperature, precipitation, wind, relative humidity, sea level pressure, potential evapotranspiration, snowfall, wave height and sea level; and for both climate and decadal timescales. Already downscaled models were first validated for the method and afterwards verified, obtaining small errors and good coherent simulations.

Extreme events of the main climate drivers were obtained and analysed for both historical and future scenarios through the combination of several statistical methods as well as through the analysis of several teleconnection patterns. Derived events such as heat waves, drought, snowstorms, storm surges, wave height among others were afterwards inferred for climate, decadal and seasonal scale.

Main results

Most important climate changes will be given by temperature, from +2°C in mean temperature up to +6°C in Barcelona or +5.5°C in Bristol and Lisbon under worst scenario, at the end of the century with respect to the present climate (1981-2010). Annual rainfall results differ depending on the region, with increases of 5% to +40% for Bristol by 2100, decreases down to -15% for Lisbon by period 2016-2035 and, with great uncertainty, no changes in Barcelona. Gathering this and temperature, mean snowfall is expected to decrease between -50% to -100% by year 2100 in both Barcelona and Bristol. Regarding sea level, Atlantic cities could experience a rise up to 50/60cm in Lisbon/Bristol respectively, with no significant changes in Barcelona.

With regard to extreme events results, patterns are alike climatic ones. Extreme temperature is expected to rise in the three cities up to +5°C \pm 2.5°C, and heat wave days up to +1000%. Heavy daily and subdaily rainfall will increase up to +30% for most common events in Barcelona and Bristol (< 2y-return). On the other hand, snowfall could increase up to +40% for 100y-return events due to greater humidity, but would strongly decrease in most common events due to greater temperature. Droughts would increment due to greater evapotranspiration. Finally, windstorms appear to increase only in Barcelona about 10 \pm 3% while 2y-return storm surge would rise in the three cities by year 2100.

1. Introduction

1.1. Context

Climate change will cause pressures and uncertainties that will pose challenges to urban living at a time when the world is becoming increasingly urbanized (ARUP & Rockefeller Foundation 2015). These challenges can affect basic urban services, such as water or energy supply, thereby stressing cities' capacity to provide of continuously functioning services for an increasing population.

In this context, RESCCUE (*RESilience to cope with Climate Change in Urban arEas*) project aims to improve urban resilience of three pilot cases, Barcelona, Lisbon and Bristol, through an assessment of climate change impacts in several sectors, and then interconnects them to assess urban resilience. This is done by obtaining projections of local future climate scenarios at different timescales and changes in related extreme events for each of the pilot cities.

1.2. Report objectives and challenges

The goal of this report is to disseminate the main results obtained from the Work Package 1 (WP1) "Climate Change Scenarios" of the RESCCUE project.

As secondary objectives, report aims to provide a general view on the individual processing steps until to obtain local extreme climate scenarios. This includes an historical hazard identification, the subsequent definition of climate drivers, the collection and quality control of the identified weather/climate variables (for both observations and climate models), application of statistical downscaling to the climate models, the analysis of the climate extreme events and the analysis of the uncertainty cascade for all the obtained outputs.

These steps drove the WP1 to several challenges. The first one was to deal with discontinuities in historical information, especially for the compilation of historical climate-related hazards (past trends and future projections according to previous studies). This was important to identify the climate drivers (i.e., the set of climates variables to work with).

The second challenge is the international nature of the project. Data collection and their corresponding quality control were required to perform from different sources of three countries. Finally, all usable instrumental data were collected from several meteorological institutions, and a set of climate model outputs were extracted from the Coupled Model Intercomparison Project Phase 5 (CMIP5).

The third challenge corresponds to the need of climate information at a local level. In this sense, the RESCCUE project opted for applying statistical downscaling methods to the climate models, according to Ribalaygua *et al.* (2013). Sub-daily precipitation time-scaling was performed for all climate models and for all time periods. Decadal prediction was performed by using two approaches, a statistical (teleconnection-based) method and a dynamical one. It is important to remark this since near-term (seasonal and decadal) predictions are highly influenced by the natural variability of the climate (yearly or multi-decadal atmospheric and ocean coupled patterns such as North Atlantic Oscillation –NAO- or Pacific Multi-Decadal Oscillation –PDO-) which causes low skill of dynamical climate models and thus need to be complemented with statistical methods. All projections were made with methods verified with observations, and afterwards their application over the data is validated.

The last challenge is to obtain climate scenarios for extreme events. The analysis of extremes in meteorology and climatology presents some problems that should always be considered, such as the definition of extreme event and their characterization due to their low occurrence, by definition, within observed series available.

By definition, low occurrence of an event is related to the tails (extremes) of a given probability distribution; since it is somehow arbitrary to establish a threshold or quantile of occurrence for a specific event (it could happen several times a year or never), return periods are used in the RESCCUE project. Each return period (T) is related to a quantile $(1 - 1/T)$ very close to 1, guaranteeing a real extreme. For the RESCCUE project it is also important to consider the potential impacts of an event in each city since it may cause, despite low-occurrence, an unappreciated impact, e.g.: snowfall in Lisbon. Because of this, specific thresholds were identified for each city and were summarised in a common criteria (Sec. 3.2).

Regarding the lack of observed extreme events and the uncertainty associated, it is advisable to use an ensemble strategy and theoretical distributions that can be fitted to the entire empirical distribution (Monjo *et al.* 2016).

1.3. Structure of the report

The report is divided into three main sections: (1) the study area and data collection, (2) the methodology used, and (3) results. In turn, these sections are structured in several points corresponding to the report objectives:

- **Study area and data collection**
 - Study area: Description of the three studied cases (Barcelona, Lisbon and Bristol).
 - Climate hazards identification: Summary of the results obtained from the climate-related hazards identification and the definition of the climate drivers for each city.
 - Data collection from observations and climate models: Description of all the data used in the study.
- **Methodology**
 - Climate simulation: Description of all downscaling methods used to simulate climate at timescales from century down to month.
 - Extreme events: Description of the definition of extremes and analysis methods of extreme events simulation.
 - Uncertainty analysis: Description of the criteria of cascading uncertainty analysis.
- **Results**
 - Results of verification and validation: Performance analysis of the methods applied to re-analysis comparing with observations (verification) and applied to climate models comparing with extended observations with re-analysis (validation).
 - Mean climate and decadal scenarios: Climate projections for next decades and for the rest of the century.
 - Extreme events scenarios: Projection of changes in extreme events according to climate and decadal scenarios and prediction of seasonal extremes.

2. Study area and data collection

About this section: Here is a summary of the study area, the identification of their climatic drivers and the required climate data collection. In case of need further or more detailed information and graphics, they can be found in the correspondent Deliverable 1.1.

2.1. Study area

Barcelona

Located at the northeast Spanish Mediterranean coast, Barcelona is a dense and compact settlement: on a surface area of 100.4 square kilometres, a population of 1.619.337 inhabitants is established, which implies a density of 15,570 inhab./km², one of the highest in Europe.

Barcelona is on a coastal plain bordered by the Collserola ridge (max. height of 512m) on the west side of the city, with tree and wetland vegetation (Figure 1). The city lies between two rivers: the Llobregat in the south and the Besòs in the north, with the entire city being water-supplied by the Ter-Llobregat watershed basin.

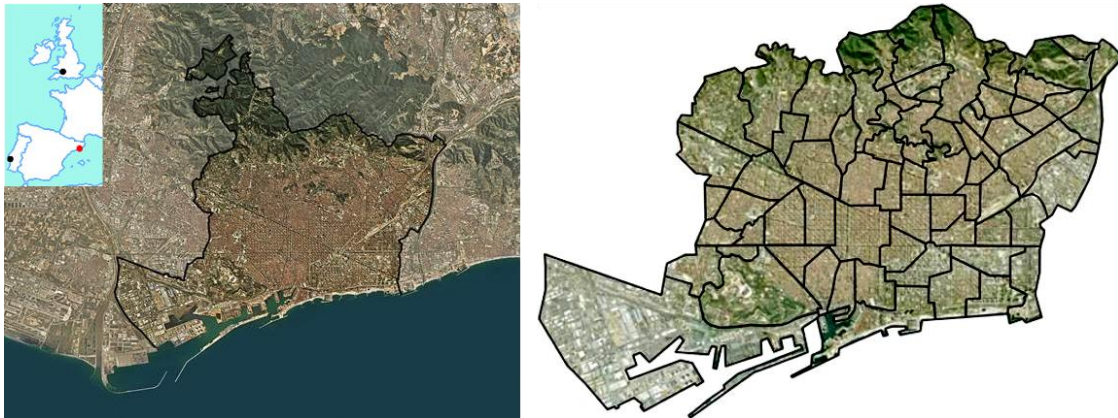


Figure 1. Barcelona urban area: a) Satellite image of the city, b) Distribution of the 73 neighbourhoods.

The city's climate is Mediterranean, with hot and humid summers and warm winters thanks to the presence of the mild Mediterranean waters, being average temperature about 16.5°C. Rainfall occurs mostly during spring and autumn, reaching a total of 598mm/year, mostly from short and intense showers; it is not rare that 50 % of the annual precipitation comes from few rainfall events. The skies tend to be clear throughout the year, counting 2,483 hours of sun and a solar radiation of 1,502 kWh/m².

Lisbon

Lisbon, the Portuguese capital, covers an area of around 100 km². It is the most populous metropolitan area of Portugal with 2,821,876 inhabitants (2011). It lies on the Atlantic coast washed by the Tagus River Estuary (named Sea of Straw) on the east and the south (Figure 2). The city is quite steep, ranging from sea level to 216.4 meters. Prone to natural disasters such as floods, windstorms or even historical tsunamis and earthquakes, Lisbon is a city shaped by different human influences over time.

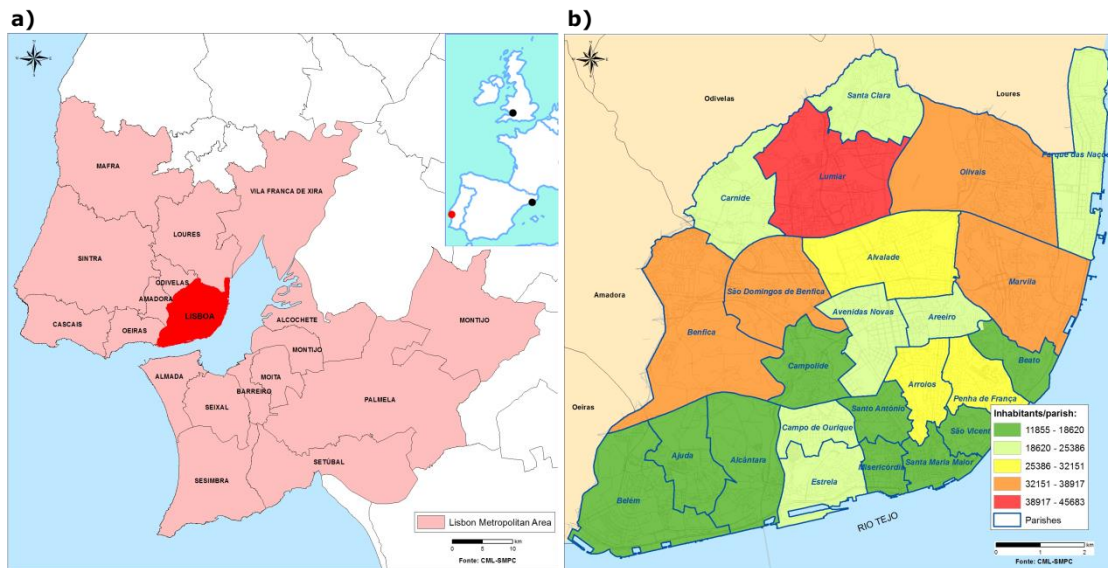


Figure 2. a) The Lisbon's Metropolitan Area. b) Lisbon's boundaries and parishes and population. Source: CML (SMPC 2016).

Lisbon enjoys a Subtropical-Mediterranean climate (Köppen climate classification: *Csa*). Temperature is characterized by short and very mild winters and warm summers with short and exceptional hot episodes. Rainfall appears mainly due to Low frontal systems during autumn and winter, with some convective episodes during spring and a dry season along summer. Thanks to its location in the Estuary, cyclonic surge is not an issue although windstorms can be severe when deep Atlantic lows approach during winter.

Bristol

Bristol city, with a population of 449,300 (2016), is the eighth most populous city in the UK, and one of the most densely populated parts of the UK. The city location, at the south-west of the island, lies over flood plains around River Avon, which flows east-west through the city, meeting River Frome in the central city and leading into Severn Estuary at Avonmouth, coastal area of the city.

The very hilly and urbanized Bristol landscape facilitates rapid runoff when heavy rainfall occurs. The convergent character of rivers and streams over Bristol (Figure 3) plus the tides of Severn Estuary (up to 14m of tidal range, second highest of the world) encroaching upstream into Bristol Channel have led to severe flood over the centre of the city and Avonmouth.

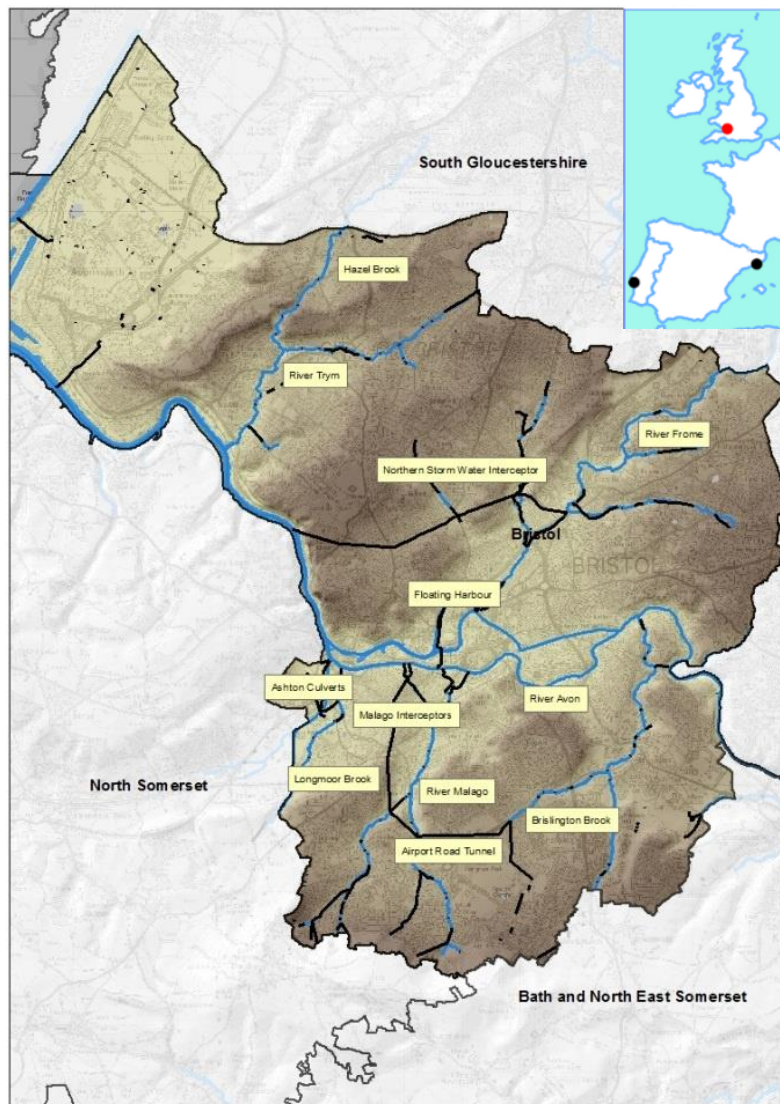


Figure 3. Identification of the significant drainage network and location of the major rivers (blue) and culverts (black) in the BCC area (excluding Avonmouth). Topography colour darkens with height.

As an island nation with temperate maritime climate, the UK is prone to variable weather conditions. Bristol’s climate, in its SW, is particularly influenced by the Atlantic conditions. Temperature tends to be mild all along the year, exceptionally getting close to 30°C in summer or below freezing point. Rainfall is frequent as drizzle all year long with the pass of frontal systems; snowfall is not rare during winter, and thunderstorms might occur in summer, with heavy rainfall. Due to its location close to Severn Estuary, storm surge and windstorms is a serious hazard for the city.

2.2. Climate hazards identification

Common criteria for the three case cities, regarding each climate hazard, are required in order to compare the natural variability and the future projections under climate change. However, before this, it is required to dispose of all the observed data, homogenized and filtered with quality controls. Since the hazard identification is prior to the data collection, several published studies and other related information (e.g.: newspapers or historic texts) were examined to identify all historical extreme events that took, and could take place, in the three cities, and

that could extend or intensify due to climate change. All identified climate and weather hazards are resumed in Table 1, being related to their correspondent weather variable and labelled regarding their importance (Climate Risk) in RESCCUE. All hazards have been evaluated considering cascading effects, and assuming constant exposure & vulnerability. To assign a Risk Level, both Probability and Urban Impact were considered and mixed into a risk matrix for each city; value showed is a general approximation for the project. Definitions of climate hazards and common thresholds taken can be found in [Section 3](#) (Extreme Events prediction).

Table 1. Data requirements for climate variables related with the identified potential hazards in each city.

Variables	City			Spatial coverage	Spatial resolution (km ² /station)	Time series length (years)	Temporal resolution	Potential hazards
	Barcelona	Lisbon	Bristol					
Temperature (mean, maximum, and minimum)	X		X	Watershed	10-1000	> 5	Daily	Drought
	X	X	X	Urban	1-10	> 5	5-10 min	Heat / Cold events and heat burst
Precipitation (liquid and solid)	X		X	Watershed	10-1000	> 5	Daily	Drought and flooding
	X	X	X	Urban	1-10	> 5	5-10 min	Flash flood and hail
Snow (observed and estimated)	X		X	Watershed	10-1000	> 5	Daily	Snowstorm
	X		X	Urban	1-10	> 5	5-10 min	Snowstorm
Wind (mean and gust)		X	X	Ocean areas	10-1000	> 20	Daily	Windstorm
	X	X	X	Urban	10	> 20	Hourly	local severe wind
Potential Evapotranspiration	X		X	Watershed	10-1000	> 5	Daily	Drought and flooding
Atmospheric pressure		X	X	Coastal waters	10-1000	> 20	Daily	Surge storm and windstorm
Sea level	X	X	X	Urban	10-100	> 20	Daily	Sea level rise and surge storm
Wave height (mean and extremes)		X	X	Urban	10-100	> 20	Hourly /daily	Storm surge and sea storm
River flow	X		X	Watershed	100-1000	> 20	Hourly /daily	River-basin flooding
Flood coverage		X	X	Urban	10 meters / pixel	> 20	Daily	Drought and flooding

2.3. Observed variables

The largest database achieved consists of temperature, precipitation, relative humidity, wind, pressure, wave height and sea level, according to the identified climate drivers (Table 1). A set of tests were applied to series (general consistency, outliers and inhomogeneities) remaining only stations with good quality of data and more than 5 years of observed variables. Tests results showed an acceptable quality for most of the datasets.

In order to simulate temperature and precipitation using statistical downscaling, time-series length of weather data were selected with at least 5 years of observations (Ribalaygua et al. 2013). For the rest of the variables, time-series were collected with at least 20 years with observations. However, analysis of extreme events required of at least one time-series (for each variable/city) with at least 50 years of length.

Due to the low availability of certain data, some variables were semi-observed, i.e. are supplemented with statistical estimations by using other observed variables. For example, potential evapotranspiration is usually simulated using temperature, solar radiation (e.g., astronomical formulae) and wind.

In the case of Barcelona, data from five different sources have been collected depending on the variable considered: AEMet (Agencia Estatal de Meteorología), SMC (Servei Meteorologic de Catalunya), Meteogrid, PE (Puertos del Estado) and BCASA (Barcelona Cicle de l'Aigua). A total of 1277 stations were gathered for the project regarding all Ter-Llobregat rivers basins within Catalonia.

For Lisbon, two weather stations with subdaily data was provided by IPMA (Instituto Português do Mar e da Atmosfera), while 6 more stations at daily scale were gathered from the NOAA-GSOD.

Regarding Bristol, observed data was obtained from four different sources: NOAA-GSOD, NRFA (National River Flow Archive), CCO (Channel Coastal Observatory) and BCC (Bristol City Council). A total of 646 weather stations were gathered considering all type of variables.

As commented above, all of the data gathered was examined so as to ensure the format and type of data as well as possible recording errors: general consistency, outliers and inhomogeneities, so as to identify all type of issues within the observed series, and afterwards decide whether the data could be homogenised or partially eliminated to make the station valid, or directly discarded. From the whole of stations gathered, a total of 817 stations were considered to be trustworthy enough to work with.

2.4. Climate models

Apart from observed data, the identified climate variables have been also collected from the ERA-Interim reanalysis and several CMIP5 model outputs, for both climate timescale (2006-2100) and decadal timescale (2016-2035) (Table 2), as well as for the historical period (1951-2005). Climate and decadal scale differ not only in the horizon considered but in the amount and type of variables available, so an ensemble strategy is taken to evaluate the uncertainty. With respect to seasonal forecast, the Climate Forecast System (CFS) model was selected to design the simulations.

Table 2 . Available CMIP5 climate models for decadal and climate experiments. The table shows the model name, the responsible institution, the model references, their spatial resolution for the AGCM, and the available RCPs for the climate simulation. The most basic run r1i1p1 was taken for all climate models except for CanESM2, for which it was the r2i1p1 run. For decadal outputs, T indicates Teleconnection-combined approach, D indicates Drift-corrected outputs, and alternative decadal experiments were taken in some case to compensate the unavailability of others.

Model	Institution	Reference	AGCM resolution (Lon×Lat)	Climate RCP				Decadal
				2.6	4.5	6.0	8.5	

ACCESS1-0	CSIRO, BOM	Bi <i>et al.</i> (2013)	1.87°×1.25°		X		X	T
BCC-CSM1-1	BCC	Xiao-Ge <i>et al.</i> (2013)	2.8°×2.8°	X	X	X	X	T,D
CanESM2	CC-CMA	Chylek <i>et al.</i> (2001)	2.8°×2.8°	X	X		X	T (CanCM4)
CMCC-CM	CMCC	Vichi <i>et al.</i> (2011) Bellucci <i>et al.</i> (2012)	0.75°×0.75°					D
CNRM-CM5	CNRM-CERFACS	Voltaire <i>et al.</i> (2013)	1.4°×1.4°	X	X		X	T,D
GFDL-ESM2M	GFDL	Dunne <i>et al.</i> (2012)	2°×2.5°	X	X	X	X	T
HADGEM2-CC	MOHC	Collins <i>et al.</i> (2008)	1.87°×1.25°		X		X	T,D
IPSL-CM5A-LR	IPSL	Dufresne <i>et al.</i> (2013)	3.75°×1.89°					D
MIROC-ESM-CHEM	JAMSTEC, AORI, NIES	Watanabe <i>et al.</i> (2011)	2.8°×2.8°	X	X	X	X	T (MIROC5)
MPI-ESM-MR	MPI-M	Marsland <i>et al.</i> (2003)	1.8°×1.8°	X	X		X	T (MPI-ESM-LR)
MRI-CGCM3	MRI	Yukimoto <i>et al.</i> (2011)	1.2°×1.2°	X	X	X	X	T,D
NorESM1-M	NCC	Bentsen <i>et al.</i> (2012), Iversen <i>et al.</i> (2012)	2.5°×1.9°	X	X	X	X	T

Acronyms:

AORI:	Atmosphere and Ocean Research Institute (Japan)
BCC:	Beijing Climate Centre, China Meteorological Administration (China)
BOM:	Bureau of Meteorology (Australia)
CC-CMA:	Canadian Centre for Climate Modelling and Analysis (Canada)
CERFACS:	Centre Européen de Recherche Formation Avancées en Calcul Scientifique (France)
COLA:	Centre for Ocean-Land-Atmosphere Studies (US)
CMCC:	Centro Euro-Mediterraneo sui Cambiamenti Climatici (Italy)
CNRM:	Centre National de Recherches Météorologiques (France)
CSIRO:	Commonwealth Scientific and Industrial Research Organisation (Australia)
IPSL:	Institut Pierre-Simon Laplace (France)
JAMSTEC:	Japan Agency for Marine-Earth Science and Technology (Japan)
GFDL:	Geophysical Fluid Dynamics Laboratory (USA)
MOHC:	Met Office Hadley Centre (UK)
NIES:	National Institute for Environmental Studies (Japan)
MPI-M:	Max Planck Institute for Meteorology (Germany)
MRI:	Meteorological Research Institute (Japan)
NCC:	Norwegian Climate Centre (Norway)
NCEP:	National Centre for Environmental Prediction (USA)

3. Methodology

About this section: Here is a summary of the methodology used to generate and analyse mean/extreme climate scenarios at a local scale for the main climate drivers identified above. In case of need further or more detailed information and graphics, they can be found in the correspondent Deliverables 1.2 and 1.3.

3.1. Climate simulation

3.1.1. General scheme

The generation of climate scenarios uses a set of statistical methods that depend on the simulated climate variable. However, a general scheme of the generation process is common for all them. To summarise the whole process scheme, we can divide the work in three parts:

(1) Method design/adaptation, (2) Methodology application (downscaled outputs) and (3) Cascade of uncertainties.

The first part, the methodology description, has been separated into several sections according to the temporal scale considered (climate, decadal or subdaily). Regarding climate and decadal, their projections for the three case cities were obtained by using several statistical downscaling methods applied to a set of CMIP5 climate models (Table 2).

The downscaling methods were verified using the ERA-Interim re-analysis as a reference for reproducing the past climate. In a similar way, the application of these methods to the available climate models was also validated according to several statistical measures.

3.1.2. Statistical downscaling methods

a) Analogy-based approach

This work uses the two-step statistical downscaling method developed by Ribalaygua *et al.* (2013). The first step is common for all simulated climate variables and it is based on an analogue stratification (Zorita *et al.* 1993): the n most similar days to the day to be downscaled are selected. The similarity between two days was measured using a weighted Euclidean distance according to three nested synoptic windows and four large-scale fields used as predictors: (1) speed and (2) direction of the geostrophic wind at 1000 hPa and (3) speed and (4) direction of the geostrophic wind at 500 hPa. For each predictor, the distance was calculated and standardised by substituting it by the closest centile of a reference population of distances for that predictor. The four predictors were finally equally weighted, while the synoptic windows had different weights.

Temperature. In the second step, a transfer function (linear by stepwise regression) is applied for $n=150$ analogous. The fact of choosing the most similar days, considering precipitation and cloudiness, reduces the non-linearity of the links between free atmosphere and surface variables. Thanks to temperature being near-normal distributed, linear regressions performs well estimating max and min values; this also obligates to take near-normal distributed predictors:

1. 1000/500 hPa thickness above the surface station.
2. 1000/850 hPa thickness above the surface station.
3. A sinusoid function of the day of the year.
4. A weighted average of the station mean daily temperatures of the ten previous days.

Two diagnostic equations are calculated (using the predicting and predictor values of the n analogous days population) and applied to estimate both daily temperatures for each station and problem day.

Precipitation. In the second step, we downscale together a group of m problem days (we use the whole days of a month). For each problem day we obtain a “preliminary precipitation amount” averaging the rain amount of its n most analogous days, so we can sort the m problem days from the highest to the lowest “preliminary precipitation amount”. And for assigning the final precipitation amount, all amounts of the $m \times n$ analogous days are sorted and clustered in m groups. Every quantity is finally assigned, orderly, to the m days previously sorted by the “preliminary precipitation amount”.

Assuming that climatic characteristics of rainfall vary little within a month, the $n \times m$ analogous days of a month can be mixed in order to obtain a better probability distribution (or Empirical Cumulative Distribution, ECDF). Therefore, the number of problem days is chosen as $m=30$; same for n considering the obtained RPS.

Other climate variables. For wind, humidity and pressure, the second step is a parametric bias correction. In order to estimate the improvement of this procedure, the bias correction was also applied to the direct model outputs (see next section). To check it a comparison was performed between the combination of both steps and the application of only the second step.

b) Parametric bias-correction

Cumulative Probability Functions. Systematic error or bias is corrected for all climate variables using parametric functions chosen from several theoretical probability distributions. For each variable, transference between observed and simulated CDF is performed throughout fitting TCDFs (*theoretical cumulative distribution function*) for each ECDF (*empirical cumulative distribution function*). Some variables behaving as almost *normal* have similar CDF's and so is enough with linear quantile mapping. For precipitation, all theoretical functions that have been considered require a *standard precipitation*, λ , defined as:

$$\lambda(p; P_0, P_1) \equiv \frac{p - P_0}{P_1} \quad \text{Eq. 1}$$

where the parameter P_0 is the most probable value and P_1 is the scale factor. Both parameters depend on the probability distribution used; in particular: Gamma, Weibull, Classical Gumbel, Reverse Gumbel and Modified Log-logistic (Monjo *et al.* 2014, 2016).

Systematic error correction. The systematic error is obtained by comparing the simulated precipitation (from climate models historical experiment) with the observed precipitation (from reference time-series). In order to correct this systematic error, it is necessary to have long time-series of reference, because the large natural variability of precipitation has a significant uncertainty associated. For that reason, we have extended the observed time series downscaling ERA40 reanalysis (1958-2000) before validation. Due to systematic error that downscaling method introduces into the extreme rainfall, we chose to correct the ECDF of each ERA40 simulation with reference to observations in the common period. This correction is based on quantile-quantile parametric transferences (Benestad 2010, Monjo *et al.* 2014). The same probabilistic correction was applied for the direct outputs and the downscaled projections simulated by the climate models.

Quantile-quantile mapping. For wind, humidity and pressure, the fitted TCDFs differ in little and therefore the transference was performed using a linear or logarithmic quantile mapping. For each model regression, an expansion in Taylor series was considered until the quadratic order.

In all, three different theoretical functions were used: linear model, simple logarithm and logarithm with offset. The best function was chosen according to the highest Pearson correlation R^2 between empirical and theoretical quantile-quantile. Thus, each original and downscaled ERA time-series was corrected with the corresponding fitted parameters.

Together with this, the Kolmogorov-Smirnov test was applied before and after corrections to analyse whether each simulated time-series is indistinguishable of the observed one (passing test according to the threshold p -value > 0.05) (Figure 4).

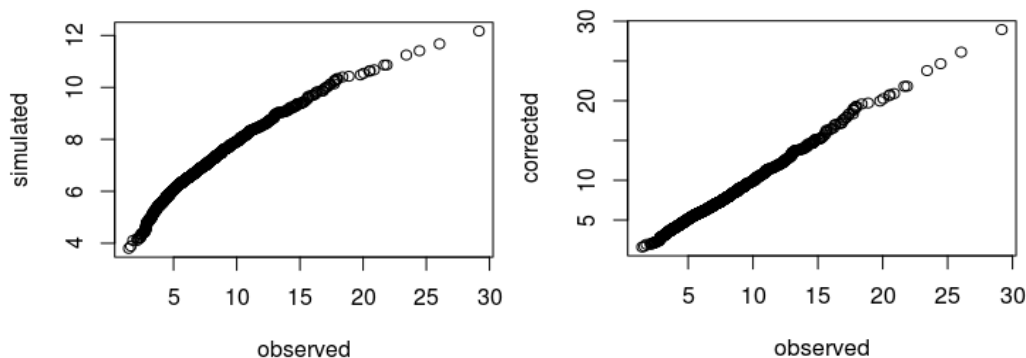


Figure 4. Example of quantile-mapping between simulated (ERA direct output) and observed time-series, for the wind (m/s) recorded in the station 03520 of Lisbon, before correction (left) and after correction (right).

c) Decadal: dynamical output correction

The data assimilation carried out for the initialization of decadal experiments causes a *drift* in the bias of the simulated variables until they are stabilized (Kim *et al.* 2012, Doblas-Reyes *et al.* 2013). The drift is produced until the model simulates enough transitory time since the beginning of the run (around 10-year horizon).

When initializing decadal experiments, the data assimilation process causes a *drift* in the simulated variables until enough transitory time passes for the model to stabilize (around 10-year horizon)(Kim *et al.* 2012, Doblas-Reyes *et al.* 2013). Considering that decadal experiments predict up to 30 years, it is necessary to consider and correct this drift.

Decadal outputs (Table 2) are collected considering ten *historical* experiments and four different *run*, which makes a total of 40 available experiments per model (except CMCC-CM with just one run and MPI-ESM-LR and MRI-CGCM3 with three). Since the bias drift depends on yearly temporal horizon, daily data are reduced into year scale and in order to keep the natural signal of the variable, *time horizon* was redefined as a temporal unit of prediction; the value at the *i*-horizon (H_{kj}) is calculated as the mean of the *i* previous years (Eq. 2).

$$H_{kj} = \frac{1}{k} \sum_{i=1}^k h_{kj} \quad \text{Eq. 2}$$

All horizons of each model are rearranged so that we compute only the ten *i*-year horizons together (where $i = 1, \dots, 10$) for each run. To correct the drift, these *i*-horizons series are standardized by using their equivalent Z-value (standard score), and then the mean (M_i) and standard deviation (S_i) are obtained as fitting parameters for each *i* (Figure 5).

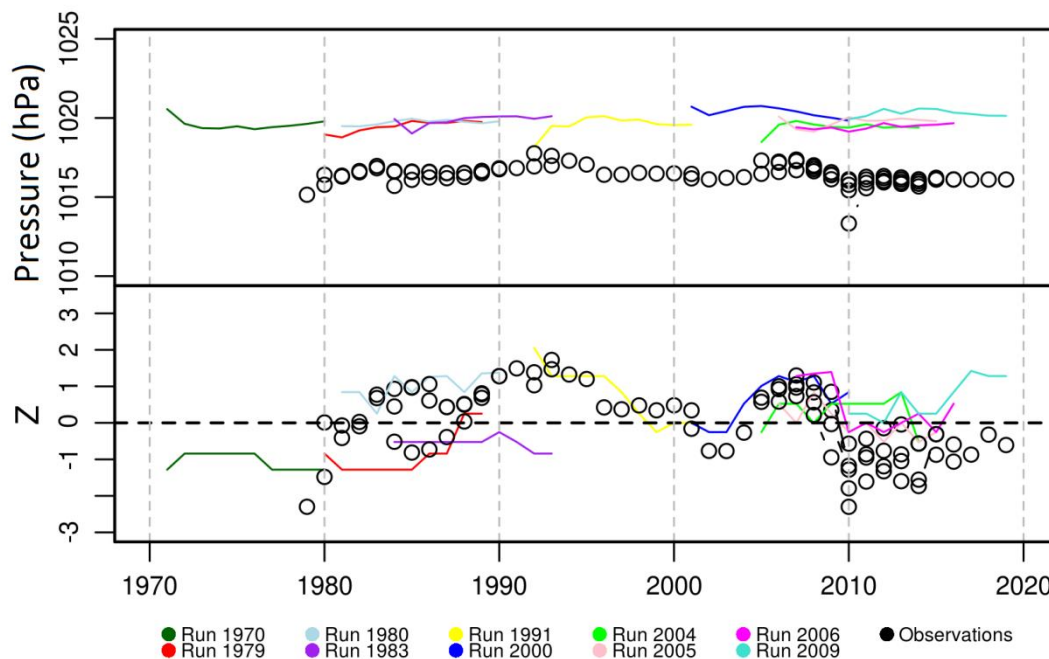


Figure 5. Example of drift-correction by standardisation. *Top:* raw decadal runs of CanCM4 model regarding Sea Level Pressure variable downscaled for the 0200E station (Barcelona). *Bottom:* the same but for normalised (Z) time-series.

The climate variables predicted using decadal simulations are: precipitation, maximum and minimum temperatures, wind and mean sea level pressure. The probability distribution considered for precipitation and wind is *log-normal* instead of *normal*. The four decadal runs (from 2005-2035) of each model are corrected using the fitting parameters of *historical* series.

Some models may not have a continuous historical time progression or have overlaps among some series. In order to obtain one complete time-series for each climate model, a merging process was performed to collapse all of the standardised runs into just one, by using the median of the values of each year. To avoid loss of signal, the resulting time-series is again standardised taking the mean and standard deviation of its 1986-2015 period (Figure 6).

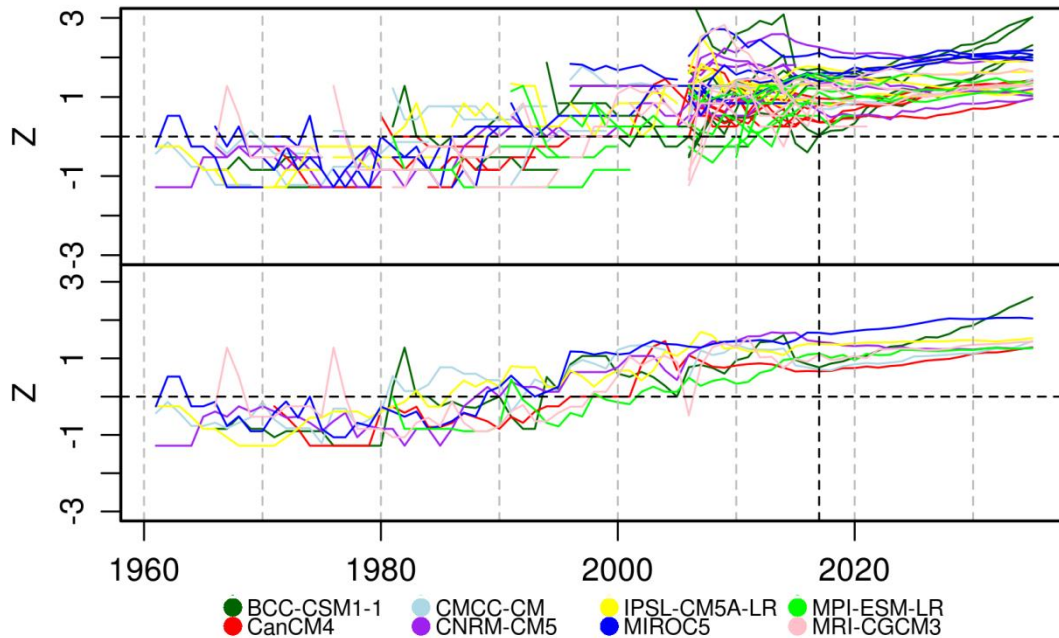


Figure 6. Example of drift-corrected output. *Top*: Z-values for minimum temperature variable in Barcelona, according all runs/experiments available for each climate model. *Bottom*: Z-values for the same variable according to the complete time-series obtained after the merge process for each climate model. Vertical dashed line marks the end of the past period (2017).

In average terms, the multi-decadal time-series represents approximately a 5-year moving average (from merging 1 to 10 horizons years). Therefore, we considered to use a 5-year moving average for the observed time-series. From this, mean and standard deviation were estimated and applied to each multi-decadal time-series so as to obtain not only the projection of the evolution of mean values, but also how trustable is that projection through the deviation of the values.

In order to obtain again daily time-series for the historical experiments and future decadal predictions, the empirical distribution function of the original daily outputs was corrected according to the mean and standard deviation (at daily scale) obtained for each drift-corrected year-horizon.

d) Decadal and seasonal: teleconnection indices

Near-term climate models based on dynamical simulation require an assimilation of the initial conditions of the climate system (Doblas-Reyes *et al.* 2013). The initial conditions of the ocean currents are little known, especially in the deep ocean, being it the most important influence on the atmosphere. In fact, decadal experiments present low skill when simulating quasi-oscillations as PDO or SAHEL (Kim *et al.* 2012, Gaetani and Mohino 2013). For this reason, a purely statistical approach was used in order to complete the decadal predictions obtained from the drift-corrected dynamical outputs. Chosen teleconnections are seen in Table 3.

Table 3. Indices and their variables considered. SST is sea surface temperature, SLP represents sea level pressure, R is rainfall, Z500 is geopotential height at 500 hPa and P700 is pressure at 700 hPa level.

Index	Start	End	Used variable	Used region	Reference
ENSOi	1870	2015	SST	El Niño 3.4 (170°W to 120°W-EQ)	NOAA (2017)
NAOi	1950	2015	P700	Ponta Delgada–Reykjavik	NOAA (2017)
AOi	1950	2015	P700	Atlantic 20°N to North Pole	NOAA (2017)
AMOi	1870	2015	SST	Atlantic 0°–60°N and 7.5°W–7.5°E	NOAA (2017)
MOi	1948	2015	SLP	Algiers–Cairo	CRU (2017)
WeMOi	1821	2013	SLP	Padua–San Fernando	UB (2017)
ULMOi-C4	1951	2015	Z500	Mediterranean: 36.5 to 42.5°N, –2.20 to 4.4°E, and 29 to 32.5°N, 14 to 25.5°E	Redolatet <i>al.</i> (2017)
PDOi	1854	2016	SST	Pacific 20°N	JISAO (2017)
SAHEL-Pi	1901	2016	R	Africa 8° to 20°N – 20°W to 10°E	JISAO (2017)
GSNW	1966	2010	SST	Atlantic 55° to 75°W - 35°N	Taylor (2011)

Acronyms:

- NOAA:** National Oceanic and Atmospheric Administration (USA).
JISAO: Joint Institute for the Study of the Atmosphere and Ocean (USA).
CRU: Climate Research Unite (UK)
UB: University of Barcelona (Spain)
ENSOi: El Niño South Oscillation index
NAOi: North Atlantic Oscillation index
AOi: Artic Oscillation index
AMOi: Atlantic Multidecadal Oscillation index
MOi: Mediterranean Oscillation index
WeMOi: Western Mediterranean Oscillation index
ULMOi: Upper Level Mediterranean Oscillation index
PDOi: Pacific Decadal Oscillation
SAHEL-Pi: Sahelian Precipitation index
GSNW: Gulf Stream North Wall index

The teleconnection-based method was applied to predict temperature and precipitation anomalies following three steps:

Firstly, the best predictors are chosen for each station according to the Akaike Information Criterion (AIC) resulting from a backward stepwise regression (Venables and Ripley 2002). The second step is a fitting process of a n -harmonic model (η) for each index. The third is to extrapolate this model for the future horizons. A *hindcast* cross-validation was performed using the n -harmonic model in order to evaluate its performance in the past (verification).

e) Sub-daily values

The calculus of sub-daily temperature was performed using a two-step statistical downscaling method. The first step consists on the selection of n most analogous days for each problem day and then averaging the sub-daily temperature recorded. To avoid the underestimation of extremes, a second step is made, consisting in a correction of the sub-daily thermal amplitude (ΔT) taking into account the maximum (T_x) and minimum temperature (T_n) simulated.

Since precipitation is a very irregular variable, it is not possible to use averages of analogous days. For this work we have used a fractal method based on the rainfall time-structure n -index (Monjo 2016). This method is a two-step process that combines transfer

functions and stochastic generation of synthetic hyetographs for individual rainfall events, alternating with realistic dry episodes.

f) Derived variables

Snowfall is a hydrometeor difficult to measure due to lack or the cost of instruments, or to its nature because of blizzards. In order to estimate climate change impacts on snowfall, the frequency and amount of snowfalls have been estimated by using the derived method of Redolat (2014). This method is an effective way to simulate days and amount of snow taking into account daily thresholds of precipitation (0.1mm), maximum and minimum temperature (9°C and 0°C respectively). Whenever these thresholds are true, precipitation is considered to be as *snow water equivalent*.

Potential evapotranspiration simulations have been calculated by using a version of the Hargreaves approach computing the monthly reference evapotranspiration (ET_0) of a grass crop based on the original Hargreaves equation (Hargreaves, 1994) that considers maximum temperature (T_x), minimum temperature (T_n) and extraterrestrial radiation (RA) as parameters (if not available, it is calculated with latitude and month).

3.2. Extreme events

3.2.1. Common criteria

a) Synthetic extreme events

After considering each city's climate, risks and requirements specified, common criteria regarding extreme events have been established in order to better define common thresholds to work with. To study extreme events evolution, **synthetic extreme (SE)** events have been designed according to a particular *return period* and drawn with isolines according to *specific thresholds*.

- **Return periods:** in order to represent all scale of extreme events possible for each city, eight periods were defined: 1, 2, 5, 10, 20, 50, 100 and 500 years. To fit data and find the proper value for each period, 2, 3 and 4-parametric versions of Gamma, Weibull, Classical Gumbel, Reverse Gumbel and Modified Log-logistic distributions (Monjo et al. 2014, 2016) functions were used.
- **Specific thresholds:** for each SE, an expected value is obtained for each station of the area, being afterwards interpolated with Thin Plate Spline (TPS) method. According to the hazard thresholds (potential impacts to particular urban services) identified by the RESCCUE partners, the isolines match with three levels, excepting some cases in Barcelona and Lisbon (Table 4).

Table 4. Specific thresholds for isolines that summarise the spatial distribution of the extreme events.

Variable	Specific threshold		
	Low	Medium	High
High temperature (°C)	30 ^{*B}	35*	40
Rainfall	1h (mm)	10 ^B	20 ^B
	12h (mm)	60*	100*
Snowfall ¹ (cm/12h)	6*	10*	14*
Wind (km/h)	70	90	130
Wave height (m)	3	5	7
Sea level + storm surge (m)	0.5	1.0	2.0

¹Snowfall intensity scaling is considered using a synthetic n-index equal to 0.3.

*Not applicable for Lisbon or variable not identified as hazard for the city.

^B Not applicable for Barcelona.

b) Baselines and horizons

A common baseline (“climate”) was selected for the project: 1986-2015, while validation period changes for each time scale: 1979-2015 for climate due to the use of ERA extended observations, 1986-2015 for decadal and 2015-2018 for seasonal due to lack of forecasts. Future horizons are established according to the nature of the method applied: climate projections extend in three 30-y period (2011-2040, 2041-2070 and 2071-2100), while decadal and seasonal have a limited horizon of application (2035 and 2018 correspondently). 2035 was also taken as a horizon for climate projections just to make comparisons with decadal scale.

It should be noted that “prediction” is used for near-term simulations since they mostly depend on natural variability, while “projections” is due to the use of RCP scenarios, mainly linked to political decisions rather than being related with numerical prediction models.

c) Spatial distribution

The spatial distribution of a SE is given by a TPS applied to all the stations within a study region. Sea variables (mean sea level and storm surge), since only one buoy was available for each port, were considered as spatially constant. Precipitation was treated with a 2-D TPS approach, while the rest of variables due to their height-dependency, were considered with a 3-D TPS approach.

d) Extreme indicators

Additional extremes indices were considered for temperature and precipitation according to several authors (Table 5).

Table 5. Criteria for additional extreme indices based on potential impacts

Index	Description	Source	Criterion	Variable	Threshold	Reference period
LHW / LCW	Long heat/cold wave	WMO (2001, 2017)	sdc 5	TX / TN	±5°C	Jul-Aug / Jan-Feb
HW / CW	Heat/cold wave	SMC (2015) and AEMET (2016)	sdc 3	TX / TN	98% / 2%	Jun-Aug / Dec-Feb
TN90 / TN10	Warm/cold night	Zhang et al. (2011)	nd	TN	90% / 10%	whole
TX90 / TX10	Warm/cold days	Zhang et al. (2011)	nd	TX	90% / 10%	whole
TR	Tropical nights	Zhang et al. (2011)	nd	TN	> 20°C	whole
FD	Frost nights	Zhang et al. (2011)	nd	TN	< 0°C	whole
CDD	dry spell duration	Zhang et al. (2011)	x	P	< 1 mm	whole
CWD	wet spell duration	Zhang et al. (2011)	x	P	≥ 1 mm	whole
SPI12, SPI24 SPEI12, SPEI24	SPI & SPEI of 12 & 24 months	McKee et al. (1993) Hargreaves (1994) Thornthwaite (1948)	pSPI	P, TA	≥ 0.1mm	whole
DPB5	Days with light rain	AMB et al. (2017)	nd	P	≥0.1&<5mm	whole
DPA50, DPA100	Days with heavy rain	AMB et al. (2017)	nd	P	>50mm >100mm	whole
CI	Concentration Index	Martin-Vide (2004)	a	P	≥ 0.1mm	whole
n, I_0	n -index	Monjo (2016)	a	P	≥ 90%	whole
Warmest period	Warmest period	FIC	x	TA	95%	whole
Summer	Warm spell	FIC	x*, s	TA	75%	whole
Winter	Cold spell	FIC	x*, s	TA	25%	whole
Coldest period	Coldest period	FIC	x	TA	5%	whole

Legend:

TX: maximum temperature
TN: minimum temperature

TA: average temperature
P: precipitation

W: wind

H: humidity

sd: sum of days with at least ... consecutive days

nd: number of days per year

x: maximum duration per year

*****: opposite spells up to 7 days are allowed

a: average per year

s: starting date, day of the year

pSPI: probability of SPI or SPEI < -1, -2, -3

3.2.2. Application to each time scale

a) *Climate and decadal climate extremes*

In order to obtain and compare extreme events, it is necessary to obtain reference SE for historic period. Real extreme events were calculated for 1986-2015 period (using bias corrected downscaled ERA-Interim -SECCION-), and SE for CMIP5 models were calculated taking historical series (1950-2005) and first ten years of RCP 4.5 (non-significant differences between RCP in this period).

Since extreme events simulated under climate change conditions can present important systematic error, future simulations are corrected obtaining first the *projected model change* subtracting simulation and their historical series, summing secondly to it the reference SE based on extended observations. Climate change has been obtained in both absolute and relative units depending on the variable. Thanks to taking as reference extended observations, mean bias and std deviation approach zero. These projections are then rearranged in function of the total change (most severe to less), and simulations corresponding to quantiles 10, 50 and 90 are extracted. Contours are plotted according to thresholds and transformed into Keyhole Markup Language (KML) format to be delivered for HAZUR® tool (Figure 7).

b) *Seasonal extremes*

As a way to improve the seasonal forecast skill, two complementary methods were applied: a mixed statistical-dynamical technique and a purely statistical teleconnection-based method.

The statistical-dynamical technique is based on the operational forecast outputs from the Climate Forecast System (CFSv4) from the NCEP. Particularly, an ensemble of 25 perturbed initial conditions is considered from the last 7 runs. This ensemble is downscaled using transfer functions among predicting (temperature, precipitation and wind) and predictors (500hPa geopotential height, 850hPa temperature, surface wind and probability of precipitation).

Teleconnection-based technique uses the partial predictability of the natural variability modes fitted to quasi-oscillation functions. This method has been adapted to seasonal forecast using training windows with shorter length.

Due to the low skill of seasonal forecast in Europe, additional techniques like extreme inference approach need to be applied (Pepler *et al.* 2015).

c) *Extreme inference approach: analogous anomalies*

Given a predicted anomaly for a month, it is possible to estimate the expected extreme (maximum/minimum) daily values according to the n most similar anomalous months in the past. The relation between a mean value and the probability distribution depends on the climate variable and the station considered. This statistical link is expected to remain during at least the next year, and therefore does not present a “stationary problem” (Ribalaygua *et al.* 2013). The similarity between pairs of months can be measured according to large-scale predictor fields or by using one-dimensional physical features. For this study the monthly anomaly is used as predictor for the similarity measure. The daily distribution of the problem month is inferred from those of the analogous ones, being the distribution then linearly interpolated through QQ method. Those quantiles are afterwards estimated from the standardized anomalies to obtain the expected seasonal extremes.

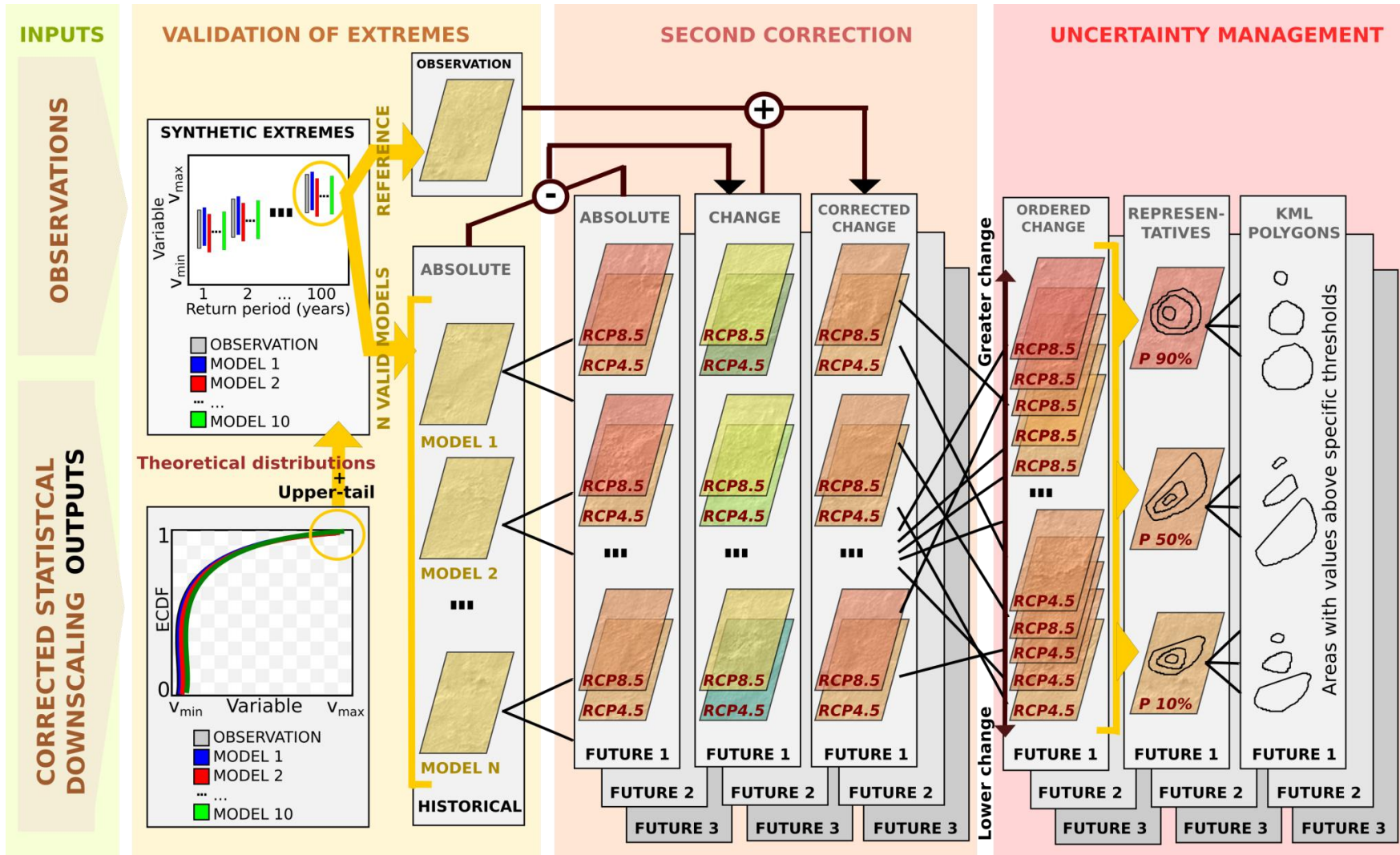


Figure 7. Detailed scheme of the method used to obtain extreme events scenarios for a climate variable in a city, according to three specific thresholds.

3.3. Uncertainty analysis

3.3.1. Verification of the methodology

The performance of all used methods were analysed comparing the observed and the simulated-by-reanalysis time-series for a past reference period, particularly 1979-2015.

The mean absolute or relative errors (MAE and MRE) were estimated for most of climate variables as a main measure of the method performance for reproducing the day-to-day weather variability, which is important so as to detect possible changes in their intensity or frequency of occurrence.

Ranking Probability Score (RPS) was calculated for precipitation simulation to compare the method ability respect to two reference predictions: the *persistence*, a prediction based on the observations from the previous day; the *climatology*, the prediction based on the climatic average for each day of the year.

Standardised mean Absolute Error (SAE) is estimated for decadal and seasonal simulations comparing their MAE with the one obtained from the *climatology* forecast.

Finally, the Kolmogorov-Smirnov (KS) test was applied to analyse the statistical significance of the similarity of the simulated probability distributions respect to the observed ones (Marsaglia *et al.* 2003). This test is useful for measuring the method ability to reproduce not only the mean distribution but also the extreme values. The KS test was also applied to measure the good performance of the bias correction.

3.3.2. Validation for the CMIP5 models

Validation process consists of evaluating the performance of applying the selected method to each climate model. Unlike the reanalysis, a *historical experiment* of a climate model does not try to reproduce the real day-to-day weather evolution in the reference period, it tries to simulate the climate variability at daily scale. So it does not make sense to use errors like MAE or RPS, but an error that depicts a more general behaviour. Moreover, since observed series present gaps, observations were extended/filled using the corrected ERA-Interim reanalysis (common period 1979-2015).

One of the main errors is the *bias* of the mean and the standard deviation, calculated as the average of the total error for each station. The non-parametric KS test is also useful to indicate if *observed* and *simulated* distributions are indistinguishable.

Bias is the main error obtained to validate simulation of extreme events for selected return periods and those from reference period 1979-2015 as a way to check regional variability.

3.3.3. Projection uncertainty

The cascade of uncertainties in climate simulation at local scale is given by four main sources: (1) The used statistical downscaling method [verification process], (2) The model/run selection and the method/model performance [validation processes], (3) the RCP scenarios considered, and (4) the climate natural variability. The last two uncertainty sources have been treated by using the ensemble strategy. That is, once bias-correction is applied to all models, a combination (ensemble) of those models provides an estimation of the uncertainty caused by the (past and future) climate variability. An ensemble is performed for each RCP scenario. This uncertainty is represented by the median of the values, plus quantiles 10th-90th to appreciate the dispersion obtained as seen in [Figure 8](#).

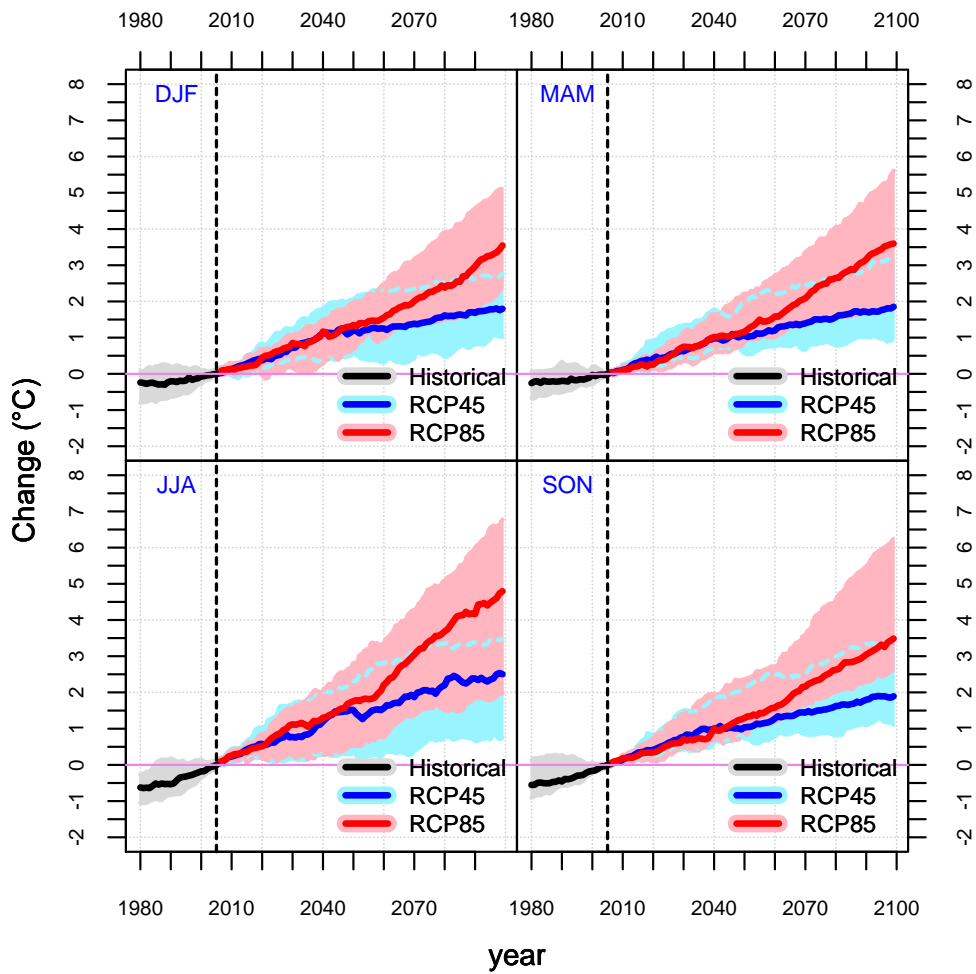


Figure 8. Example of ensemble strategy. Panel shows seasonal climate projections of changes in temperature for a random city. The ensemble median (solid lines) and the 10th–90th percentile values (shaded areas) are displayed. The vertical dashed line marks the end of the Historical data (2005).

4. Results of verification and validation

About this section: Here is a summary of verification and validation results for the whole of the methods and processes performed in the project. In case of need further or more detailed information and graphics, they can be found in the correspondent Deliverables 1.2 and 1.3.

4.1. Mean climate

4.1.1. Verification

All climate variables are adequately simulated by the downscaling methods except the sea level in Barcelona due to errors in salinity, although the downscaling method does not require it and therefore validation process is not affected by this uncertainty.

Daily maximum/minimum temperature showed bias and MAE respectively lower than 0.2°C and 2°C, with accurate sub-daily values (MAE around 1°C in winter and 1.5°C in summer). Precipitation presented a BIAS lower than 10%. Statistics of wind, relative humidity and pressure showed that the analogous method obtained the lowest MAE and almost zero BIAS. All of the variables passed the Kolmogorov-Smirnov test for the daily and sub-daily distributions. These results confirm that the analogous method is a powerful tool to simulate accurately these variables.

Regarding the teleconnection method, temperature is well simulated at all time scales for Barcelona and Bristol, although Lisbon presented predictability only at >10 years horizon. Precipitation is only predictable for horizons equal or greater than 20 years. Gathering both variables, optimum forecast is obtained for >20years horizon.

4.1.2. Climate models validation

After applying the verified method to models and performing the correspondent BIAS correction, the analysis of obtained KS p-values show that all climate model outputs are valid for temperature (except for GFDL-ESM2M), wind, ETP, wave height and meteorological surge (only available for Bristol), with some exceptions for precipitation, snowfall and sea level rise.

Precipitation, due to its nature, showed some issues for several models, although HADGEM2-CC presented major problems for the hydrological area of Barcelona and Bristol, and therefore was been removed for climate projections (Table 6). Errors in temperature are propagated in the estimation of snowfall, even after correction, and therefore GFDL-ESM2M cannot be used for this variable. Sea level rise is generally badly simulated by climate models for the three cities, even after bias correction. Only a few models passed most of the statistical test. Therefore, results of sea level projections should be used with great care.

Table 6. Summary of the validation for the downscaled climate models according to the previous assessment.

Variable	City	Model									
		ACCESS1-0	BCC-CSM1-1	CanESM2	CNRM-CM5	GFDL-ESM2M	HADGEM2-CC	MIROC-ESM-CHEM	MPI-ESM-MR	MRI-CGCM3	NorESM1-M
Temperature	Barcelona	Green	Green	Green	Green	Yellow	Green	Green	Green	Green	Green
	Lisboa	Green	Green	Green	Green	Yellow	Green	Green	Green	Green	Green
	Bristol	Green	Green	Green	Green	Yellow	Green	Green	Green	Green	Green
Precipitation	Barcelona	Green	Green	Green	Green	Green	Red	Green	Green	Green	Green
	Lisboa	Green	Yellow	Yellow	Yellow	Yellow	Yellow	Green	Yellow	Green	Green
	Bristol	Green	Yellow	Yellow	Green	Green	Red	Green	Green	Yellow	Yellow
Wind	Barcelona	Green	Green	Green	Green	Green	Green	Green	Green	Green	Green
	Lisboa	Green	Green	Green	Green	Green	Green	Green	Green	Green	Green
	Bristol	Green	Green	Green	Green	Green	Green	Green	Green	Green	Green
Snowfall	Barcelona	Green	Green	Green	Green	Red	Green	Green	Green	Green	Green
	Bristol	Green	Green	Green	Green	Red	Green	Green	Green	Red	Green
ETP	Barcelona	Green	Green	Green	Green	Green	Green	Green	Green	Green	Green
	Lisboa	Green	Green	Green	Green	Green	Green	Green	Green	Green	Green
	Bristol	Green	Green	Green	Green	Green	Green	Green	Green	Green	Green
RH	Barcelona	Green	Green	Green	Green	Green	Green	Green	Green	Green	Green
	Bristol	Green	Green	Green	Green	Green	Green	Green	Green	Green	Green
Sea level	Barcelona	Yellow	Grey	Yellow	Yellow	Red	Yellow	Yellow	Green	Yellow	Yellow
	Lisboa	Yellow	Grey	Yellow	Yellow	Yellow	Yellow	Yellow	Green	Yellow	Yellow
	Bristol	Yellow	Grey	Yellow	Green	Yellow	Yellow	Yellow	Yellow	Yellow	Yellow
Wave height	Barcelona	Green	Green	Green	Green	Green	Green	Green	Green	Green	Green
	Bristol	Green	Green	Green	Green	Green	Green	Green	Green	Green	Green
Surge	Bristol	Green	Green	Green	Green	Green	Green	Green	Green	Green	Green
Pressure	Bristol	Green	Green	Green	Green	Green	Green	Green	Green	Green	Green

Legend:

	Valid according to less than 50% of statistics
	Valid according to more than 50% and less than 70% of statistics
	Valid according to more than 70% of statistics
	Not available

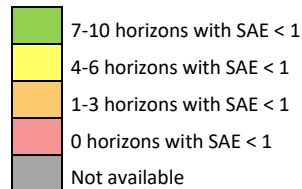
4.1.3. Decadal dynamical method validation

As a way to summarize the decadal validation process, a classification of the climate models has been performed. All conclusions regarding SAE analysis are reflected in [Table 7](#). A code of colours has been adopted according to the number of horizons well simulated by the decadal historical simulations of 10 horizons. Only those models that could achieve a yellow/green colour after counting were considered trustworthy enough to be used for the decadal forecasts, while those obtaining a red/orange colour were discarded for next steps.

Table 7. Summary of the validation for the drift-corrected decadal outputs according to the SAE criterion. The process counts the number of consecutive horizons where the model achieves a SAE < 1.

Climate model	Pressure			Precipitation			Maximum temperature			Minimum temperature			Snowfall			Wind		
	Barcelona	Bristol	Lisbon	Barcelona	Bristol	Lisbon	Barcelona	Bristol	Lisbon	Barcelona	Bristol	Lisbon	Barcelona	Bristol	Lisbon	Barcelona	Bristol	Lisbon
BCC-CSM1-1	Green	Red	Red	Green	Red	Yellow	Green	Red	Red	Green	Red	Red	Grey	Grey	Grey	Grey	Grey	Grey
CanCM4	Yellow	Green	Orange	Red	Green	Red	Green	Green	Green	Green	Green	Green	Yellow	Yellow	Red	Red	Red	Red
CMCC-CM	Yellow	Green	Red	Red	Red	Red	Green	Green	Green	Green	Green	Yellow	Red	Orange	Yellow	Green	Yellow	Yellow
CNRM-CM5	Red	Red	Yellow	Red	Yellow	Red	Green	Orange	Yellow	Green	Yellow	Green	Grey	Grey	Grey	Grey	Grey	Grey
IPSL-CM5A-LR	Yellow	Green	Green	Orange	Orange	Yellow	Green	Green	Green	Green	Green	Green	Red	Green	Red	Yellow	Orange	Orange
MIROC5	Yellow	Yellow	Green	Red	Orange	Yellow	Green	Green	Green	Green	Green	Green	Red	Green	Red	Red	Yellow	Red
MPI-ESM-LR	Red	Red	Red	Red	Red	Red	Green	Yellow	Green	Green	Yellow	Green	Grey	Grey	Grey	Grey	Grey	Grey
MRI-CGCM3	Red	Red	Red	Red	Red	Red	Green	Green	Yellow	Green	Green	Yellow	Grey	Grey	Grey	Grey	Grey	Grey

Legend:



Both temperature variables are fairly good estimated by almost every model for the three RESCCUE cities, with green colours widely present. This was expected due to temperature nature. Wind, pressure and precipitation presented worse results due to their more chaotic daily distribution, with none or just a few models able to represent properly the variable historical behaviour, what exposes future projections to possible systematic errors of the model. Snowfall is directly simulated by few decadal experiments with poor results, thus it was calculated as a derived variable to be afterwards applied.

4.2. Extreme events

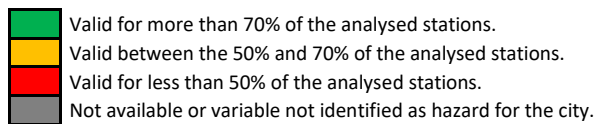
4.2.1. Validation for the climate scale

The analysis of the BIAS between extreme values simulated from downscaled corrected models and those from extended observations are summarized in Table 3. Alike in verification, a colour code was applied to explain results: green/orange colours were assigned to those results that proved to be good for at least 50% of the stations involved in the area of study, and thus considered valid; red colour implies a discard of the model. Validation was performed for the eight return periods, although just three were represented as example of near/mid/long periods.

Results tend, as expected, to worsen with higher return periods. Extreme temperatures present only acceptable results in few climate models for Lisbon and Bristol, while most of them passed tests for Barcelona. Wind gust extremes presented problems when simulated in the Barcelona area, whereas wave height got difficult to predict for Lisbon at high return periods. The rest of variables perform correctly under most of climate models (Table 8).

Table 8. Summary of the validation process for long-term climate simulations downscaled for the three cities.

Return period	CMIP5 climatic models	Max. Temp.			Rainfall			Snowfall			Wind gust			Storm surge			Wave height		
		Barcelona	Bristol	Lisbon	Barcelona	Bristol	Lisbon	Barcelona	Bristol	Lisbon	Barcelona	Bristol	Lisbon	Barcelona	Bristol	Lisbon	Barcelona	Bristol	Lisbon
2 years	ACCESS1-0	Green	Red	Green	Green	Green	Green	Green	Green	Green	Green	Green	Green	Green	Green	Green	Green	Green	Green
	BCC-CSM1-1	Green	Yellow	Green	Green	Red	Green	Green	Green	Green	Green	Green	Green	Green	Green	Green	Green	Green	Green
	CanESM2	Green	Green	Yellow	Green	Green	Green	Green	Green	Green	Green	Green	Green	Green	Green	Green	Green	Green	Green
	CNRM-CM5	Green	Green	Green	Green	Green	Green	Red	Green	Green	Green	Green	Green	Green	Green	Green	Green	Green	Green
	GFDL-ESM2M	Green	Red	Red	Green	Green	Green	Green	Green	Green	Green	Green	Green	Green	Green	Green	Green	Green	Green
	HADGEM2-CC	Green	Yellow	Red	Red	Green	Green	Green	Green	Green	Green	Green	Green	Green	Green	Green	Green	Green	Green
	MIROC-ESM-CHEM	Red	Yellow	Green	Green	Green	Green	Green	Green	Green	Yellow	Green	Green	Green	Green	Green	Green	Green	Green
	MPI-ESM-MR	Green	Red	Yellow	Green	Green	Green	Green	Green	Green	Green	Green	Green	Green	Green	Green	Green	Green	Green
	MRI-CGCM3	Green	Green	Green	Green	Green	Green	Green	Green	Green	Green	Green	Green	Green	Green	Green	Green	Green	Green
	NorESM1	Green	Red	Green	Green	Green	Green	Green	Green	Green	Green	Green	Green	Green	Green	Green	Green	Green	Green
10 years	ACCESS1-0	Yellow	Red	Red	Green	Green	Green	Green	Green	Green	Green	Green	Green	Green	Green	Green	Green	Green	Green
	BCC-CSM1-1	Green	Red	Yellow	Green	Red	Green	Green	Green	Green	Green	Green	Green	Green	Green	Green	Green	Green	Yellow
	CanESM2	Green	Red	Red	Green	Green	Green	Green	Green	Green	Green	Green	Green	Green	Green	Green	Green	Green	Yellow
	CNRM-CM5	Yellow	Green	Yellow	Green	Green	Green	Yellow	Green	Green	Green	Green	Green	Green	Green	Green	Green	Green	Green
	GFDL-ESM2M	Green	Red	Red	Green	Green	Green	Green	Green	Green	Green	Green	Green	Green	Green	Green	Green	Green	Yellow
	HADGEM2-CC	Green	Yellow	Red	Red	Green	Green	Green	Green	Green	Yellow	Green	Green	Green	Green	Green	Green	Green	Green
	MIROC-ESM-CHEM	Red	Green	Green	Green	Green	Green	Green	Green	Green	Red	Green	Green	Green	Green	Green	Green	Green	Yellow
	MPI-ESM-MR	Green	Red	Yellow	Green	Green	Green	Green	Green	Green	Green	Green	Green	Green	Green	Green	Green	Green	Green
	MRI-CGCM3	Green	Green	Yellow	Green	Green	Green	Green	Green	Green	Green	Green	Green	Green	Green	Green	Green	Green	Green
	NorESM1	Red	Red	Green	Green	Green	Green	Green	Green	Green	Green	Green	Green	Green	Green	Green	Green	Green	Green
100 years	ACCESS1-0	Yellow	Red	Red	Green	Green	Green	Yellow	Green	Green	Green	Green	Green	Green	Green	Green	Green	Green	Red
	BCC-CSM1-1	Green	Red	Green	Green	Red	Green	Green	Green	Green	Green	Green	Green	Green	Green	Green	Green	Green	Red
	CanESM2	Green	Red	Red	Green	Green	Green	Green	Green	Green	Red	Yellow	Green	Yellow	Green	Green	Green	Green	Red
	CNRM-CM5	Red	Yellow	Yellow	Green	Green	Green	Green	Green	Red	Green	Yellow	Green	Green	Green	Green	Green	Green	Yellow
	GFDL-ESM2M	Green	Red	Red	Green	Green	Green	Green	Green	Green	Yellow	Green	Green	Green	Green	Green	Green	Green	Red
	HADGEM2-CC	Green	Yellow	Red	Red	Green	Green	Red	Green	Green	Red	Green	Yellow	Green	Yellow	Green	Green	Green	Yellow
	MIROC-ESM-CHEM	Red	Green	Green	Green	Green	Green	Green	Green	Green	Red	Green	Green	Green	Yellow	Green	Green	Red	
	MPI-ESM-MR	Green	Red	Yellow	Green	Green	Green	Green	Green	Green	Yellow	Green	Yellow	Green	Green	Green	Green	Green	Green
	MRI-CGCM3	Green	Green	Yellow	Green	Green	Green	Green	Green	Green	Yellow	Green	Green	Green	Green	Green	Green	Green	Green
	NorESM1	Red	Red	Yellow	Green	Green	Green	Green	Green	Green	Red	Green	Green	Green	Green	Green	Green	Green	Green



4.2.2. Validation of decadal simulations

Validation of both teleconnection and dynamical methods is here represented. Temperature is well simulated by most of the drift-corrected decadal outputs considering low and high return periods (Table 9) while rainfall is better simulated by decadal teleconnections combined with climate models. Wind gust extremes are not correctly simulated for Lisbon, and snowfall presented problems in Barcelona for the highest return periods. Models that did not pass verification appear as dark grey slots.

Table 9. Summary of the validation process for near-term (decadal) climate simulations according to two approaches: Combination of teleconnections with climate models (left) and drift-corrected decadal outputs (right).

Return period	Downscaled models combined with decadal teleconnections	Maximum temperature			Rainfall			Snowfall			Wind Gust		
		Barcelona	Bristol	Lisbon	Barcelona	Bristol	Lisbon	Barcelona	Bristol	Lisbon	Barcelona	Bristol	Lisbon
2 years	ACCESS1-0	Yellow	Red	Red	Green	Green	Green	Grey	Grey	Grey	Grey	Grey	Grey
	BCC-CSM1-1	Green	Red	Green	Green	Green	Green	Grey	Grey	Grey	Grey	Grey	Grey
	CanESM2	Yellow	Green	Yellow	Green	Green	Green	Grey	Grey	Grey	Grey	Grey	Grey
	CNRM-CM5	Green	Green	Green	Green	Green	Green	Grey	Grey	Grey	Grey	Grey	Grey
	GFDL-ESM2M	Yellow	Red	Red	Green	Green	Green	Grey	Grey	Grey	Grey	Grey	Grey
	HADGEM2-CC	Green	Red	Red	Green	Green	Green	Grey	Grey	Grey	Grey	Grey	Grey
	MIROC-ESM-CHEM	Red	Yellow	Green	Green	Green	Green	Grey	Grey	Grey	Grey	Grey	Grey
	MPI-ESM-MR	Green	Red	Yellow	Green	Green	Green	Grey	Grey	Grey	Grey	Grey	Grey
	MRI-CGCM3	Green	Green	Yellow	Green	Green	Green	Grey	Grey	Grey	Grey	Grey	Grey
	NorESM1	Red	Red	Green	Green	Green	Green	Grey	Grey	Grey	Grey	Grey	Grey
	10 years	ACCESS1-0	Yellow	Red	Red	Green	Green	Green	Grey	Grey	Grey	Grey	Grey
BCC-CSM1-1		Green	Red	Green	Green	Green	Green	Grey	Grey	Grey	Grey	Grey	Grey
CanESM2		Yellow	Green	Red	Green	Green	Green	Grey	Grey	Grey	Grey	Grey	Grey
CNRM-CM5		Yellow	Yellow	Green	Green	Green	Green	Grey	Grey	Grey	Grey	Grey	Grey
GFDL-ESM2M		Green	Red	Red	Green	Green	Green	Grey	Grey	Grey	Grey	Grey	Grey
HADGEM2-CC		Green	Red	Red	Green	Green	Green	Grey	Grey	Grey	Grey	Grey	Grey
MIROC-ESM-CHEM		Red	Yellow	Green	Green	Green	Green	Grey	Grey	Grey	Grey	Grey	Grey
MPI-ESM-MR		Green	Red	Yellow	Green	Green	Green	Grey	Grey	Grey	Grey	Grey	Grey
MRI-CGCM3		Green	Green	Red	Green	Green	Green	Grey	Grey	Grey	Grey	Grey	Grey
NorESM1		Red	Red	Green	Green	Green	Green	Grey	Grey	Grey	Grey	Grey	Grey
100 years		ACCESS1-0	Yellow	Red	Red	Green	Green	Green	Grey	Grey	Grey	Grey	Grey
	BCC-CSM1-1	Green	Red	Green	Green	Green	Green	Grey	Grey	Grey	Grey	Grey	Grey
	CanESM2	Green	Red	Red	Green	Green	Green	Grey	Grey	Grey	Grey	Grey	Grey
	CNRM-CM5	Red	Yellow	Green	Green	Green	Green	Grey	Grey	Grey	Grey	Grey	Grey
	GFDL-ESM2M	Yellow	Red	Red	Green	Green	Green	Grey	Grey	Grey	Grey	Grey	Grey
	HADGEM2-CC	Yellow	Yellow	Red	Green	Green	Green	Grey	Grey	Grey	Grey	Grey	Grey
	MIROC-ESM-CHEM	Red	Red	Green	Green	Green	Green	Grey	Grey	Grey	Grey	Grey	Grey
	MPI-ESM-MR	Green	Red	Yellow	Green	Green	Green	Grey	Grey	Grey	Grey	Grey	Grey
	MRI-CGCM3	Green	Green	Red	Green	Green	Green	Grey	Grey	Grey	Grey	Grey	Grey
	NorESM1	Red	Red	Red	Green	Green	Green	Grey	Grey	Grey	Grey	Grey	Grey

Return period	CMIP5 models considered for drift-corrected decadal outputs	Maximum temperature			Rainfall			Snowfall			Wind Gust			
		Barcelona	Bristol	Lisbon	Barcelona	Bristol	Lisbon	Barcelona	Bristol	Lisbon	Barcelona	Bristol	Lisbon	
2 years	BCC-CSM1-1	Green	Grey	Grey	Green	Grey	Green	Grey	Grey	Grey	Grey	Grey	Grey	
	CanCM4	Green	Green	Green	Grey	Green	Grey	Yellow	Green	Grey	Grey	Grey	Grey	
	CMCC-CM	Green	Green	Red	Grey	Grey	Grey	Grey	Grey	Grey	Green	Green	Red	
	CNRM-CM5	Green	Grey	Green	Grey	Yellow	Grey	Grey	Grey	Grey	Grey	Grey	Grey	
	IPSL-CM5A-LR	Green	Red	Green	Grey	Grey	Green	Grey	Green	Grey	Green	Grey	Grey	
	MIROC5	Green	Green	Green	Grey	Green	Green	Grey	Green	Grey	Grey	Red	Grey	
	MPI-ESM-LR	Green	Green	Red	Grey	Grey	Grey	Grey	Grey	Grey	Grey	Grey	Grey	
	MRI-CGCM3	Green	Green	Green	Grey	Grey	Grey	Grey	Grey	Grey	Grey	Grey	Grey	
	10 years	BCC-CSM1-1	Green	Grey	Grey	Green	Grey	Green	Grey	Grey	Grey	Grey	Grey	Grey
		CanCM4	Green	Green	Green	Grey	Green	Grey	Red	Green	Grey	Grey	Grey	Grey
		CMCC-CM	Green	Green	Red	Grey	Grey	Grey	Grey	Grey	Grey	Green	Green	Red
CNRM-CM5		Green	Grey	Green	Grey	Yellow	Grey	Grey	Grey	Grey	Grey	Grey	Grey	
IPSL-CM5A-LR		Green	Red	Red	Grey	Grey	Green	Grey	Green	Grey	Green	Grey	Grey	
MIROC5		Green	Green	Green	Grey	Green	Green	Grey	Green	Grey	Grey	Red	Grey	
MPI-ESM-LR		Red	Green	Red	Grey	Grey	Grey	Grey	Grey	Grey	Grey	Grey	Grey	
MRI-CGCM3		Yellow	Red	Red	Grey	Grey	Grey	Grey	Grey	Grey	Grey	Grey	Grey	
100 years		BCC-CSM1-1	Green	Grey	Grey	Green	Grey	Green	Grey	Grey	Grey	Grey	Grey	Grey
		CanCM4	Green	Green	Green	Grey	Green	Grey	Red	Green	Grey	Grey	Grey	Grey
		CMCC-CM	Green	Yellow	Green	Grey	Grey	Grey	Grey	Grey	Grey	Green	Green	Red
	CNRM-CM5	Green	Grey	Yellow	Grey	Green	Grey	Grey	Grey	Grey	Grey	Grey	Grey	
	IPSL-CM5A-LR	Yellow	Green	Red	Grey	Grey	Green	Grey	Green	Grey	Green	Grey	Grey	
	MIROC5	Green	Green	Green	Grey	Green	Green	Grey	Green	Grey	Grey	Red	Grey	
	MPI-ESM-LR	Red	Green	Red	Grey	Grey	Grey	Grey	Grey	Grey	Grey	Grey	Grey	
	MRI-CGCM3	Red	Red	Red	Grey	Grey	Grey	Grey	Grey	Grey	Grey	Grey	Grey	

■	Valid for more than 70% of the analysed stations
■	Valid between the 50% and 70% of the analysed stations
■	Valid for less than 50% of the analysed stations
■	Model did not pass the main climate tests for the city
■	Variable not identified as hazard for the city

4.2.3. Seasonal validation

The general result for the seasonal hindcast is that the model performance when simulating extreme precipitation is more adequate in the teleconnection-based approach, while temperature is best simulated using drift-corrected dynamical outputs (Table 10).

Table 10. Summary of the validation process for the seasonal forecast.

Method	Time horizon	Maximum Temperature			Precipitation		
		Barcelona	Bristol	Lisbon	Barcelona	Bristol	Lisbon
Downscaled CFSv4	1 month	Green	Green	Green	Red	Red	Red
	3 months	Green	Green	Green	Red	Red	Red
	6 months	Green	Green	Green	Red	Red	Red
	12 months	Grey	Grey	Grey	Grey	Grey	Grey
Teleconnections	1 month	Red	Red	Red	Green	Yellow	Yellow
	3 months	Yellow	Yellow	Yellow	Green	Green	Yellow
	6 months	Green	Yellow	Red	Yellow	Green	Green
	12 months	Green	Yellow	Yellow	Green	Red	Green

- Valid for more than 70% of the analysed cases
- Valid between the 50% and 70% of the analysed cases
- Valid for less than 50% of the analysed cases
- Horizon not available for the method

5. Mean climate and decadal scenarios

About this section: Here is a summary of climate projections and decadal predictions obtained in the project, detailed city by city. In case of need further or more detailed information and graphics, they can be found in the correspondent deliverables 1.2 and 1.3.

5.1. Barcelona

The most important change in the future climate of Barcelona is given by the temperature rise. For the next two decades temperature would not rise more than +1.5°C according to both decadal predictions; however, by the end of century, annual mean temperature could rise between 2.2°C and 5.8°C in Barcelona up to 6.5°C in Ter-Llobregat system (Table 11).

With a high uncertainty level, no significant changes are expected in annual rainfall. However, less water reserves are expected because snowfall could decrease down to 100% in Ter-Llobregat system by 2100. Moreover, an increment of the potential evapotranspiration (up to +0.6 mm/day, i.e. 27%) would cause a greater water stress.

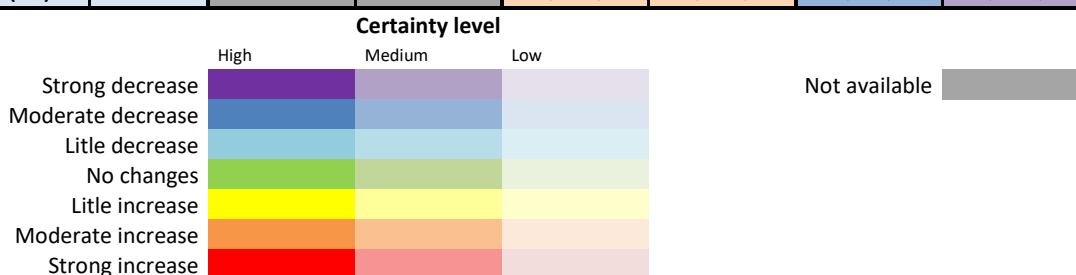
Wind speed could be reduced down to 0.6 m/s according to the RCP8.5 and the decadal forecast, especially in autumn. The mean wave height also could be reduced down to 10 cm by 2100. This is coherent with the projected increase of the mean pressure, probably due to a greater prevalence of high-pressure systems to the detriment of the low-pressure areas.

Finally, sea level rise is projected with a remarkable uncertainty level, but the most probable scenario (depending on the RCP) corresponds to +20 cm (RCP4.5) or +30 cm (RCP8.5) in Barcelona.

Table 11. Summary of mean changes projected to 2035 and 2100 in Barcelona according the decadal and climate models.

Climate variable	Spatial coverage	2035				2100	
		Decadal predictions vs 1986-2015		Climate change vs 1979-2015		Climate change vs 1979-2015	
		Tele-connections (2016-2035)	Drift-corrections (2016-2035)	RCP4.5 (2006-2035)	RCP8.5 (2006-2035)	RCP4.5 (2071-2100)	RCP8.5 (2071-2100)
Temperature (°C)	Regional	(+0.1/+1.5)	(+0.6/+1.0)	(+0.4/+1.6)	(+0.4/+1.5)	(+1.0/+3.5)	(+2.3/+6.5)
	Urban	(+0.2/+1.5)	(+0.2/+1.0)	(+0.5/+1.5)	(+0.5/+1.5)	(+1.0/+3.0)	(+2.2/+5.8)
Precipitation (%)	Regional	(-10/+10)	(-5/+5)	(-10/+10)	(-15/+10)	(-15/+15)	(-20/+25)
	Urban	(-10/+10)	(-5/+5)	(-15/+10)	(-20/+10)	(-15/+10)	(-30/+30)
Wind (m/s)	Regional		(-0.6/+0.0)	(-0.5/+0.5)	(-0.5/+0.5)	(-0.5/+0.5)	(-0.5/+0.5)
	Urban		(-0.6/+0.0)	(-0.2/+0.2)	(-0.2/+0.2)	(-0.2/+0.2)	(-0.2/+0.2)
Snowfall (%)	Regional	(-80/-0)	(-80/-0)	(-60/-8)	(-70/-6)	(-90/-50)	(-100/-85)
	Urban	(-80/-0)	(-70/-0)	(-100/-20)	(-100/+10)	(-100/-80)	(-100/-95)
ETP (%)	Regional	(+0/+5)	(+1/+5)	(+1/+6)	(+0/+6)	(+0/+14)	(+0/+27)
RH (%)	Urban			(-0.5/+0.5)	(-0.5/+0.5)	(-2.0/+1.0)	(-3.0/+1.0)
Sea level (cm)	Urban			(+0/+30)	(+0/+30)	(+10/+40)	(+10/+50)
Wave height (cm)	Urban			(+0/+4)	(+0/+4)	(-5/-0)	(-10/-0)

Legend:



5.2. Lisbon

Temperature could rise in Lisbon between 2°C and 5.5°C under the scenario RCP8.5, and between 1°C and 3.5°C under the scenario RCP4.5 (Table 12). For the next two decades, the warming will be lower than 1°C according to the decadal forecasting.

For the same period (2016-2035), a possible decrease in annual rainfall down to -15% is expected according to teleconnection method. By the end of the century, non-significant changes are expected in rainfall but with a high uncertainty level.

Sea level could experience an increase up to +60 cm by the end of the century under the RCP8.5, where ETP would rise up to +22%; both variables however present a high uncertainty level. The rest of climate variables would not undergo significant changes.

Table 12. Summary of mean changes projected to 2035 and 2100 in Lisbon according the decadal and climate models.

Climate variable	Spatial coverage	2035				2100	
		Decadal predictions vs 1986-2015		Climate change vs 1979-2015		Climate change vs 1979-2015	
		Tele-connections (2016-2035)	Drift-corrections (2016-2035)	RCP4.5 (2006-2035)	RCP8.5 (2006-2035)	RCP4.5 (2071-2100)	RCP8.5 (2071-2100)
Temperature (°C)	Urban	(+0.0/+1.0)	(+0.0/+0.3)	(+0.3/+1.0)	(+0.3/+1.2)	(+1.0/+3.0)	(+2.0/+5.4)
Precipitation (%)	Urban	(-15/-5)	(-15/-0)	(-10/+15)	(-15/+15)	(-10/+15)	(-15/+15)
Wind (m/s)	Urban		(-0.1/-0.0)	(-0.6/+0.2)	(-0.4/+0.4)	(-0.4/+0.2)	(-0.4/+0.2)
RH (%)	Urban			(-0.5/+0.5)	(-0.5/+0.5)	(-1.5/+0.5)	(-2.0/+0.0)
ETP (%)	Regional	(+0/+8)	(+0/+7)	(+0/+9)	(+0/+10)	(+0/+12)	(+0/+22)
Sea level (cm)	Urban			(+5/+15)	(+5/+15)	(+20/+40)	(+30/+60)

Legend:

	Certainty level			
	High	Medium	Low	Not available
Strong decrease				
Moderate decrease				
Little decrease				
No changes				
Little increase				
Moderate increase				
Strong increase				

5.3. Bristol

RCP8.5 projection estimates increases between 2.3°C and 5.6°C in 2100 while the RCP4.5 projection presents a smoother trend, showing rises between 1.0°C and 3.0°C by the end of the century (Table 13). Decadal predictions leave temperature rise in a maximum of +2°C.

In the case of Bristol, a significant increase in annual precipitation is projected between +10% and +40% by 2100 under the RCP8.5 scenario. The increase is less significant (between +5 and +20%) under the RCP4.5 scenario. No significant change is appreciated in decadal scale.

Despite the increment of precipitation, snowfall could decrease between 40% and 100% by the end of century according to RCP8.5 (due to the great warming). Moreover, a greater water stress is expected because of the increase in ETP up to 0.4 mm/day (22%) by the 2100.

A sea level rise up to 50 and 60 cm is expected in Bristol, respectively under the RCP4.5 and RCP8.5 scenario. The rest of the climate variables would not experience significant changes.

Table 13. Summary of mean changes projected to 2035 and 2100 in Bristol according the decadal and climate models.

Climate variable	Spatial coverage	2035				2100	
		Decadal predictions vs 1986-2015		Climate change vs 1979-2015		Climate change vs 1979-2015	
		Tele-connections (2016-2035)	Drift-corrections (2016-2035)	RCP4.5 (2006-2035)	RCP8.5 (2006-2035)	RCP4.5 (2071-2100)	RCP8.5 (2071-2100)
Temperature (°C)	Regional	(+0.4/+2.0)	(+0.0/+1.0)	(+0.4/+1.4)	(+0.4/+1.5)	(+0.7/+3.1)	(+1.7/+5.8)
	Urban	(+0.4/+1.9)	(+0.5/+0.8)	(+0.5/+1.3)	(+0.3/+1.4)	(+1.0/+3.0)	(+2.3/+5.6)
Precipitation (%)	Regional	(+0/+30)	(-1/+2)	(-2/+15)	(-5/+15)	(+5/+20)	(+10/+40)
	Urban	(-5/+10)	(-1/+2)	(-2/+15)	(-5/+15)	(+5/+20)	(+10/+40)
Wind (m/s)	Regional		(-0.2/+0.2)	(-0.4/+0.4)	(-0.4/+0.4)	(-0.4/+0.4)	(-0.4/+0.4)
	Urban		(-0.1/+0.1)	(-0.4/+0.4)	(-0.4/+0.4)	(-0.4/+0.4)	(-0.4/+0.4)
Snowfall (%)	Regional	(-70/-0)	(-60/-0)	(-55/-0)	(-50/+10)	(-90/+15)	(-100/-40)
	Urban	(-70/-0)	(-60/-0)	(-60/-15)	(-50/-15)	(-80/-50)	(-100/-60)
ETP (%)	Regional	(+0/+5)	(-1/+1)	(+1/+6)	(+1/+6)	(+0/+11)	(+0/+22)
RH (%)	Urban			(-0.5/+0.5)	(-0.5/+0.5)	(-2.0/+0.5)	(-2.0/+0.5)
Sea level (cm)	Urban			(+5/+15)	(+5/+15)	(+25/+50)	(+30/+60)
Wave height (cm)	Urban			(-1/+1)	(-1/+1)	(-1/+2)	(-1/+2)
Surge (%)	Urban			(-2/+1)	(-2/+3)	(-1/+3)	(-2/+2)
Pressure (hPa)	Regional		(-1.0/+0.5)	(-1.0/+1.5)	(-1.0/+1.5)	(-1.0/+2.0)	(-0.5/+2.0)



6. Extreme events scenarios

About this section: Here is a summary of changes in extreme events obtained in the project. In the case of need of further or more detailed information and graphics, they can be found in the correspondent deliverable 1.4.

As a way to depict most important variables and their associated most important change along the century (the worst case scenario), a Compass Rose of extreme events has been designed to summarise most of results for the three case cities: Barcelona (blue), Lisbon (red) and Bristol (green) (Figure 9).

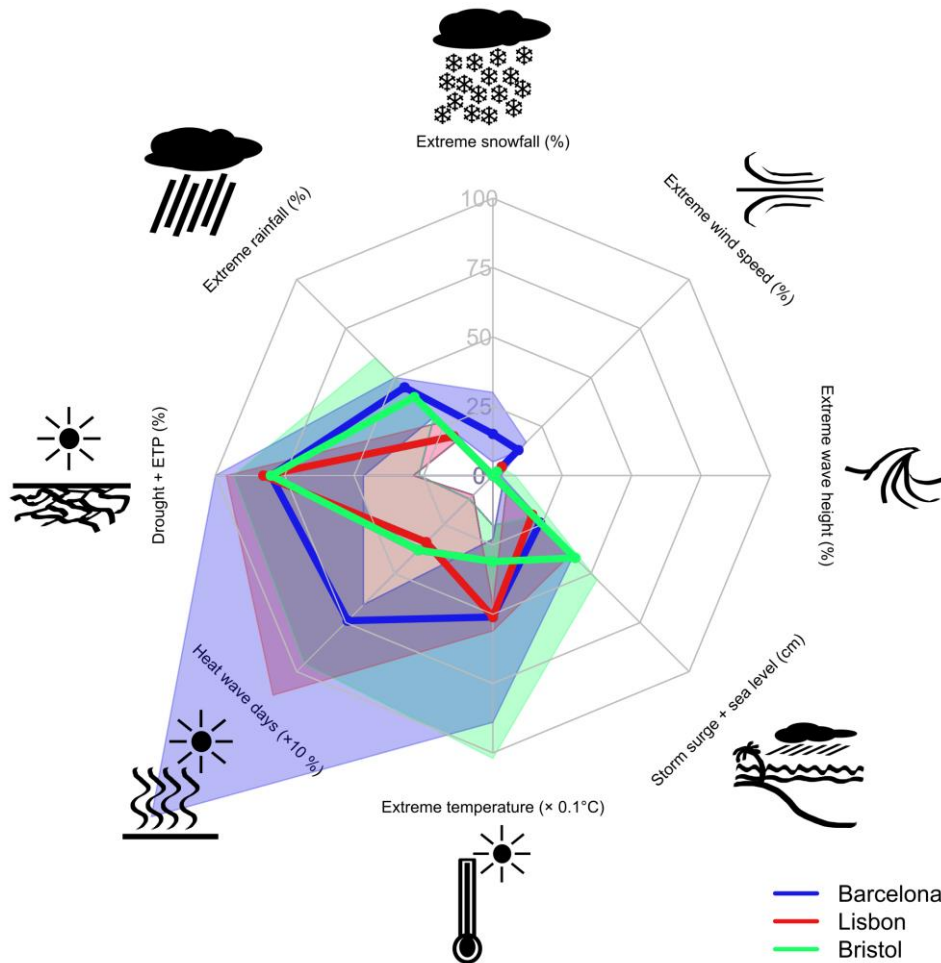


Figure 9. Extremes Compass Rose for Barcelona, Lisbon and Bristol: Maximum point change in climate extreme events along the century taking into account return periods between 2 and 100 years. The centre represents no changes and the edge corresponds to an increase of 100% for every variable except for heat wave days (border is +1000%), storm surge (border is 100cm) and extreme temperature (border is +10°C). Thick lines represent the median scenario and the shaded area is the uncertainty region (95%).

Some of the variables represented have been analysed more in deep and changes have been resumed in tables for different return periods (2, 10 and 100) and time scales (decadal and climate) for a further detail of obtained changes. Both table and rose are discussed next for each city (see following subsections).

6.1. Barcelona

Going into detail for Barcelona, 100y-return extreme temperature presents no changes for decadal scale. However, climate scale shows a rise of temperature for all time horizons up to +5.1°C by the period 2071-2100 (Table 14, Figure 10), with uncertainty going from +2.3°C up to +8.9°C in the worst-case scenario.

Table 14. Summary of changes in extremes values for Barcelona according to decadal and climate models.

Variable	Return period (years)	Observed	Decadal forecast	Relative change		
		1986-2015	2016-2035	2011-2040	2041-2070	2071-2100
Maximum Temperature	2	33.7 °C	+0.1 (-0.3/+0.4)	+1.1 °C (+0.5/+2.1)	+2.7 °C (+1.7/+4.4)	+3.8 °C (+2.2/+7.5)
	10	34.7 °C	-0.0 °C (-0.1/+0.4)	+1.0 °C (+0.5/+2.1)	+2.7 °C (+1.6/+4.2)	+4.2 °C (+2.0/+8.2)
	100	37.1 °C	-0.8 °C (-0.9/+1.1)	+1.2 °C (0.4 /+2.6)	+2.8 °C (1.2 /+5.5)	+5.1 °C (+2.3/+8.9)
12h Precipitation	2	80 mm	+0 % (-10/+10)	+7 % (-1/+20)	+19 % (-2/+30)	+30 % (+8/+40)
	10	100 mm	+1 % (-10/+10)	+9 % (+1/+20)	+20 % (+5/+30)	+40 % (+8/+40)
	100	130 mm	-0 % (-10/+10)	+6 % (+3/+18)	+30 % (+6/+60)	+45 % (+30/+50)
Wind Gust	2	85 km/h	+6 % (+4/+7)	-4 % (-7/+3)	-3 % (-4/+10)	-3 % (-5/+7)
	10	93 km/h	+10 % (+8/+12)	-0.1 % (-2/+8)	-0.3 % (-1/+12)	-0.7 % (-1.6/+9)
	100	103 km/h	+13 % (+12/+17)	+2.5 % (-0.1/+3.8)	+1.5 % (-1.7/+3.0)	+2.0 % (-1/+4)
12h Snowfall	2	14 mm		-70 % (-90/-60)	-70 % (-90/-60)	-70 % (-80/-50)
	10	20 mm		-62 % (-66/-46)	-67 % (-76/-43)	-66 % (-75/+58)
	100	29 mm		+40 % (+5.0/ +50)	+30 % (-10/+110)	+60 % (-3/+300)
Storm surge + sea level rise	2	0.54 m		5% (-30/+10)	30% (-10/+40)	45% (+10/+75)
	10	0.74 m		0% (-30/+5)	15% (-15/+20)	30% (+0/+50)
	100	1.15 m		-10% (-30/+0)	0% (-20/+10)	10% (-15/+25)
Wave Height	2	6.6 m		-1 % (-7/+3)	-4 % (-7/+1.5)	-4 % (-10/+0.3)
	10	7.7 m		-4 % (-12/+1.4)	-5 % (-11/0.7)	-5 % (-10/+0.4)
	100	9.2 m		-13 % (-20/-6)	-12 % (-22/-2)	-11 % (-20/-1)

Not available

Significant increase P > 95%
 Not significant increase 50% < P < 95%
 Not significant changes P < 50%
 Not significant decrease 50% < P < 95%
 Significant decrease P > 95%

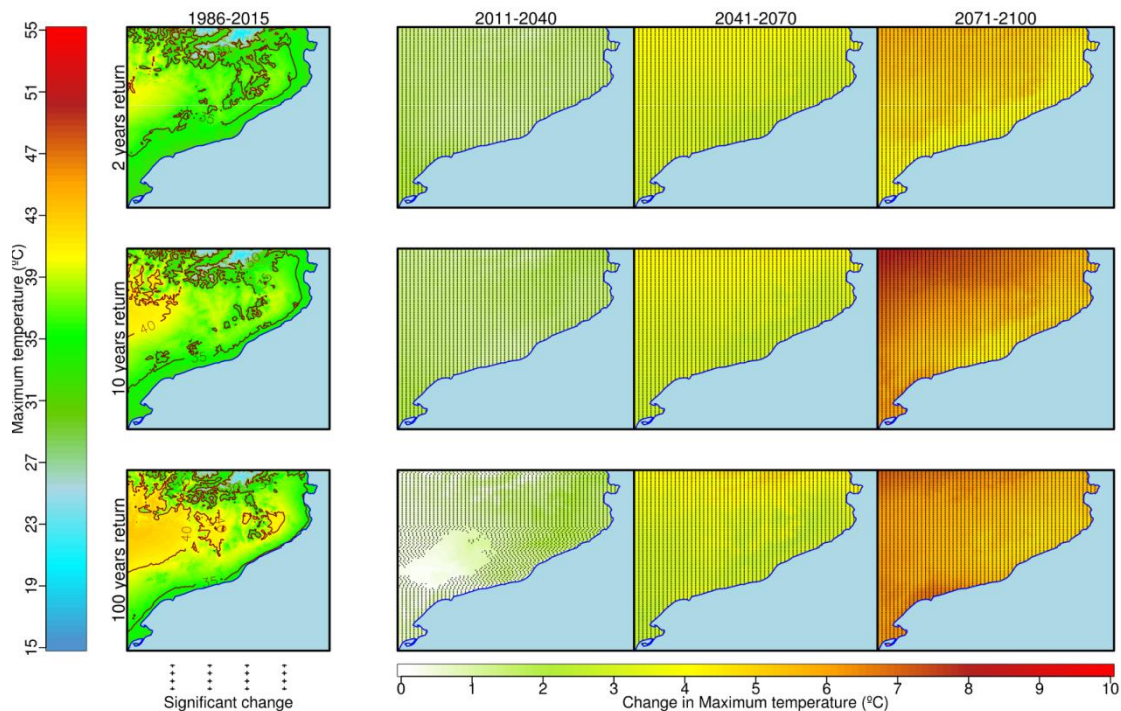


Figure 10. Multi-model median scenario of changes in extreme events of maximum temperature projected for the Ter-Llobregat system. Changes correspond to 2, 10 and 100-year return periods (rows) and three future time periods (2011-2040, 2041-2070 and 2071-2100, second to fourth column) with respect to the reference period 1986-2015 (first column).

Meanwhile, heat wave days will suffer a great increase of 750%, with little uncertainty below median but high above it with the worst-case scenario pointing to an increase of up to 1500%. This increase in both temperature and heat waves will have associated an increase in hydrological drought (from SPEI), with values rising from +50% up to +100% with an expected value of +75% by 2100 (Figure 9).

Extreme rainfall events, which are common in the Mediterranean climate of Barcelona, are presumed to notably increase up to a 30% at subdaily scale, regarding 100-y return period events, for next 2011-2040 period despite big uncertainty. This uncertainty gets remarkably reduced by 2071-2100 period, with increases of up to 20% (Figure 11). Daily precipitation is expected to increase a 45% with remarkable little uncertainty, ranging increases from 30 to 50%. These results are reached by 2071-2100 period regarding 100-year return period events. Most frequent events also present increases in extreme values, although less pronounced. In the case of snowfall only an increase in these events is expected for long return-period events (100 years), being only significant for 2011-2040 period, with a median in the change of 40% ranging values from 5% to 50% in the amount of surface snow measured. For more frequent return periods a decrease in snowfall is expected.

Storm surge (combined with sea level rise) present no significant changes for 2011-2070 period due to a greater frequency of stable atmospheric situations (high pressure systems). However, most of the downscaled climate models project an increase in 2y-return events of storm surge (+ sea level rise) between +10% and +75% (median of 45%) for the last time period (2071-2100).

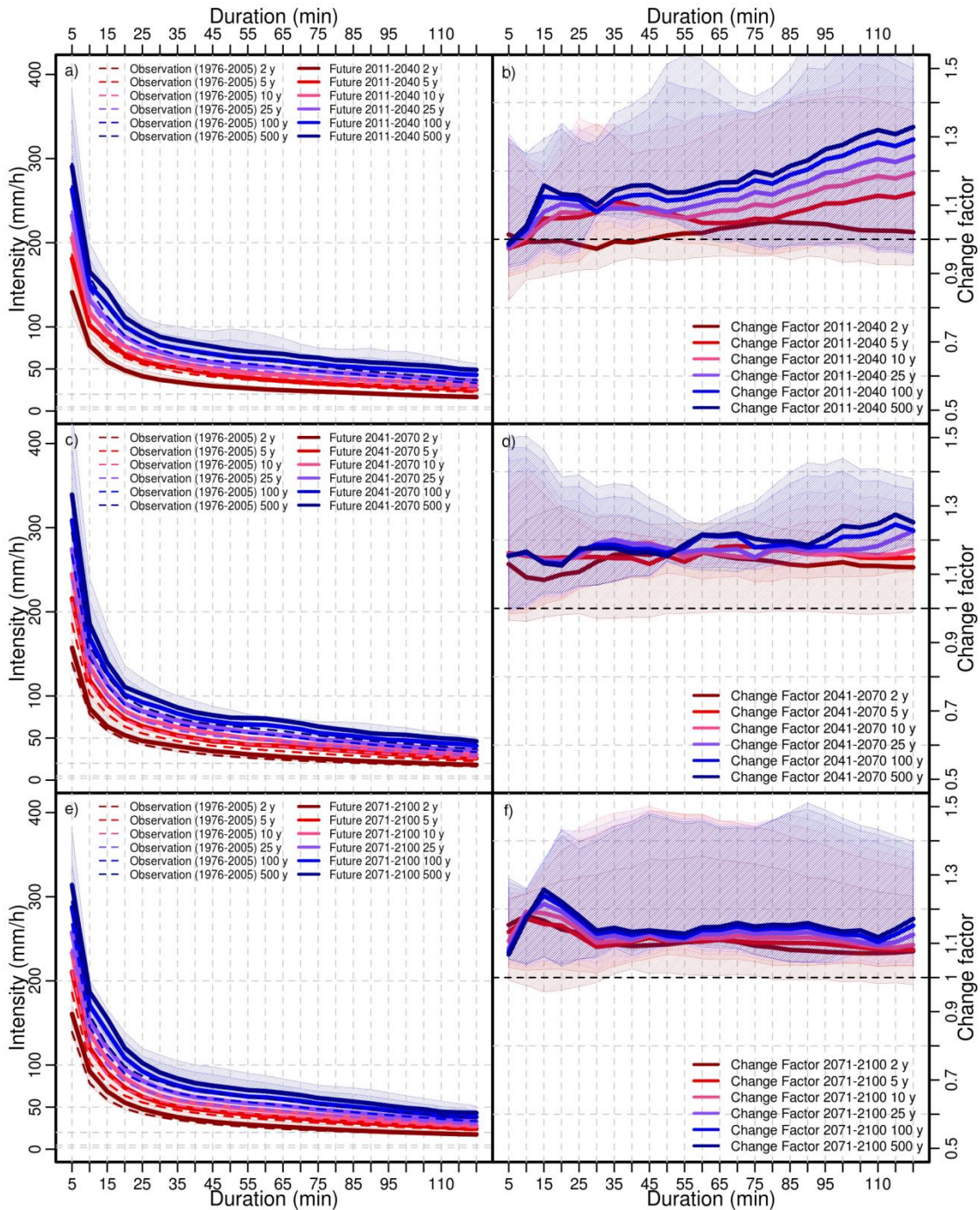


Figure 11. Projected IDF curves for the Barcelona city (Facultat de Física Station) according to absolute values (left panels) and the change factor (right panels) for three future time periods: 2011-2040 (a, b), 2041-2070 (c, d) and 2071-2100 (e, f). Dashed coloured lines correspond to observations while thick ones represent simulations. Shaded areas represent uncertainty between quantiles 10th and 90th.

6.2. Lisbon

Extreme temperature peak values are presumed to significantly increase for all time periods of the century and all return periods in Lisbon. Highest increases are expected by the end of the century, with a median increase of +5.1°C and little uncertainty for 100-year events (from +4.7°C to 5.6°C), although the biggest increase is expected for 2-year events, with a median of +5.0°C and a spread ranging from 1.9°C up to 7.2°C (Table 15 Figure 12). Heat wave days are also presumed to suffer from a great increase in extreme values, with a median of 250% increase but with high uncertainty level (from 100% up to 1000%)(Table 15, Figure 9).

Table 15. Summary of changes in extremes values for Lisbon municipality according to the decadal and climate models.

Variable	Return period (years)	Observed 1986-2015	Decadal forecast 2016-2035	Relative change		
				2011-2040	2041-2070	2071-2100
Maximum Temperature	2	34.9 °C	+0.2 °C (-0.3/+0.5)	+1.2 °C (+1.3/+2.1)	+1.9 °C (+1.7/+3.5)	+5.0 °C (+1.9/+7.2)
	10	38.9 °C	-0.2 °C (-0.4/+0.5)	+1.2 °C (+0.5/+2.0)	+2.1 °C (+2.3/+3.8)	+4.2 °C (+4.0/+5.5)
	100	40.7 °C	-0.1 °C (-0.9/+0.4)	+1.8 °C (0.75/+3.1)	+3.3 °C (+1.0/+3.4)	+5.1 °C (+4.7/+5.6)
1h Precipitation	2	17 mm	+5 % (-6/+12)	+8 % (+5/+10)	+10 % (+7/+13)	+14 % (+11/+16)
	10	29 mm	+8 % (-6/+18)	+7 % (+3/+12)	+14 % (+10/+16)	+17 % (+14/+23)
	100	40 mm	+9% (-10/+16)	+8 % (+4/+13)	+15 % (+11/+18)	+19 % (+17/+26)
Wind Gust	2	68.0 km/h		-5.3 % (-5.4/+0.4)	-0.4 % (-6.4/+2.5)	-2.0 % (-6.1/-0.8)
	10	95 km/h		+1.5 % (+0.5/+1.6)	+1.6 % (-0.3/+2)	+0.7 % (-0.4/+3)
	100	116 km/h		+4.5 % (+2.1/+4.6)	+2.4 % (+1.2/+5.0)	+4.2 % (-0.9/+4.9)
Storm surge + sea leve rise	2	0.67 m		-10% (-15/+5)	10% (+0/+30)	30% (+10/+60)
	10	0.88 m		-10% (-25/-0)	0% (-10/+15)	20% (+0/+40)
	100	1.26 mm		-20% (-30/-10)	-10% (-20/+5)	-5% (-15/+20)

Not available 

Significant increase	P > 95%
Not significant increase	50% < P < 95%
Not significant changes	P < 50%
Not significant decrease	50% < P < 95%
Significant decrease	P > 95%

Hydrological drought values behave the same, with a great median increase of +80% but incertitude ranging from 0% up to +90%. However, pluviometric drought (only-dependent of the rainfall or SPI) is not expected to change

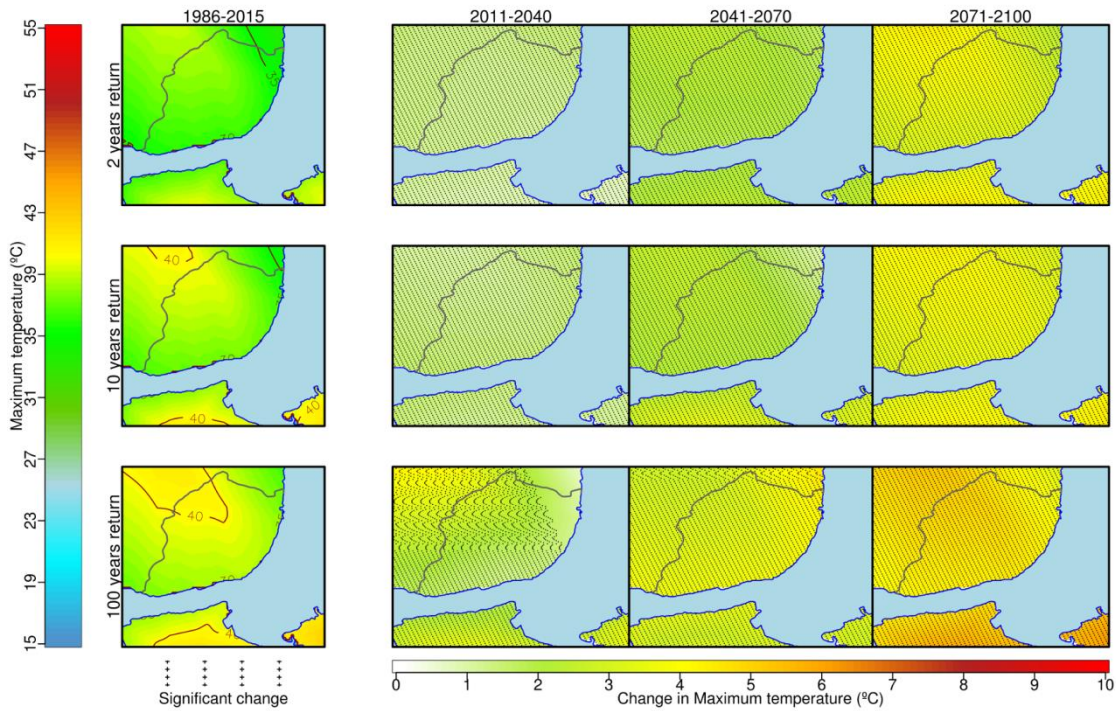


Figure 12. Multi-model median scenario of changes in extreme events of maximum temperature for the Lisbon area, according to 2, 10 and 100-year return periods (rows) and for three future time periods (2011-2040, 2041-2070 and 2071-2100, second to fourth column) with respect to the reference period 1986-2015 (first column).

On the other hand, extreme hourly rainfall could rise up to +20% (Figure 13) by the period 2071-2100, more specifically the most frequent events (2 to 10-y return period), although all events present positive changes for the three time horizons. Extreme daily precipitation, on the other hand, does not show significant changes. Regarding the rest of the variables, wind gusts would also increment for high return periods, but only during the next decades, up to +4.5%. For the end of century, storm surge could increase up to +30% (median scenario) for the 2-year return events.

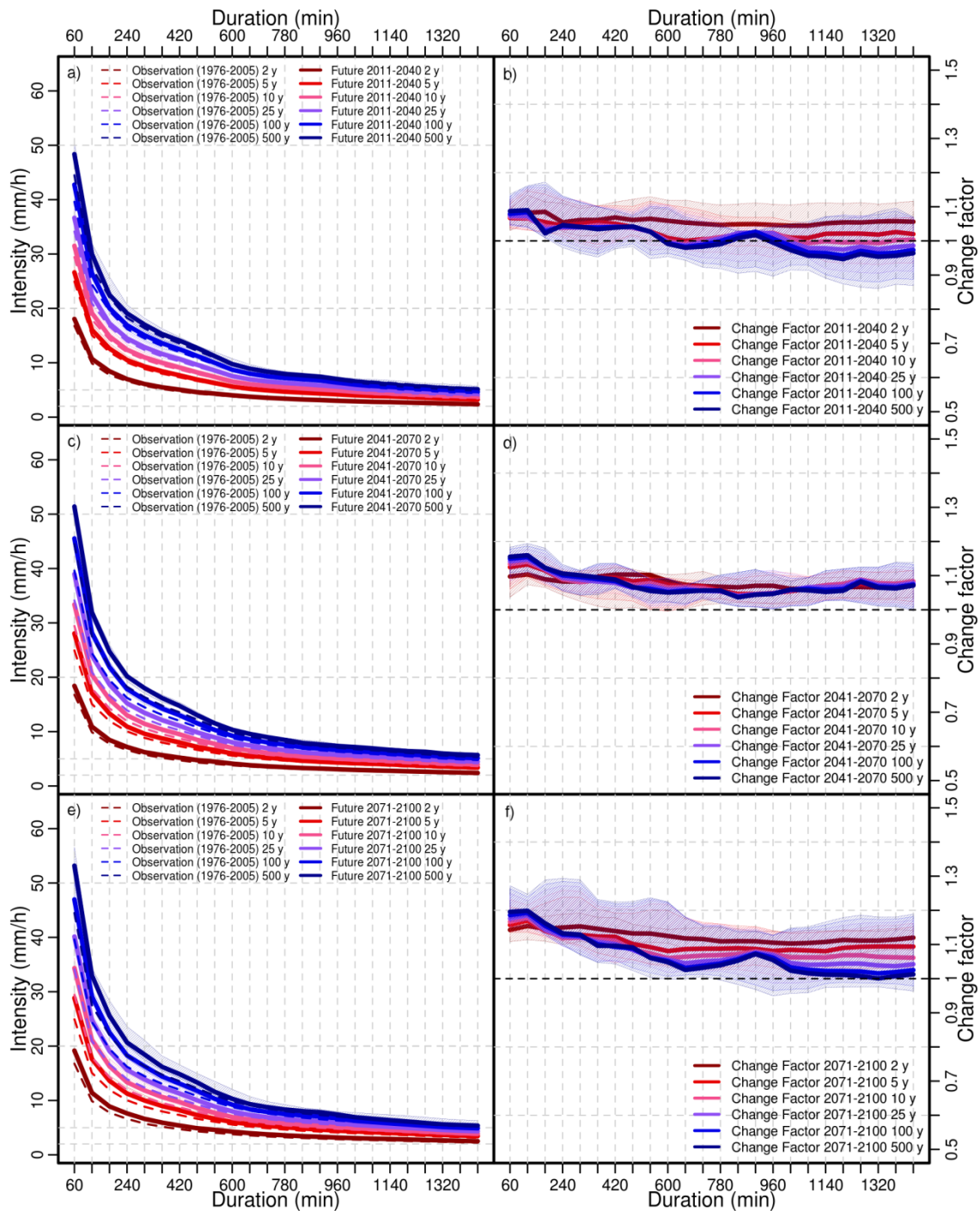


Figure 13. Projected IDF curves for the Lisbon Portela airport (station No. 085790) according to absolute values (left panels) and the change factor (right panels) for three future time periods: 2011-2040 (a, b), 2041-2070 (c, d) and 2071-2100 (e, f). Dashed coloured lines correspond to observations while thick ones represent simulations. Shaded areas represent uncertainty between quantiles 10th and 90th.

6.3. Bristol

Regarding temperature in Bristol, extreme values are presumed to raise about +3.1°C by 2100, although with a considerable uncertainty level between that goes from +1.8°C to a remarkable +10.2°C under the worst-case scenario, showing thus a huge spread (Table 16, Figure 8).

Table 16. Summary of changes in extremes values for Bristol according to the decadal and climate models.

Variable	Return period (years)	Observed	Decadal forecast	Relative change		
			2016-2035	2011-2040	2041-2070	2071-2100
Maximum Temperature	2	28.9 °C	+0.3 °C (-2.1/+0.9)	+1.3 °C (-0.4/+2.5)	+3.8 °C (+1.0/+4.6)	+3.3 °C (+0.6/+9.8)
	10	30.9 °C	-0.5 °C (-2.6/+1.0)	+1.3 °C (-0.3/+2.13)	+3.8 °C (+1.8/+5.3)	+3.2 °C (+0.9/+9.8)
	100	32.8 °C	-0 °C (-1.8/+0.8)	+1.4 °C (+0.18/+4.3)	+3.9 °C (+2.3/+6.2)	+3.1 °C (+1.8/+10.2)
12h Precipitation	2	27 mm	+ 2 % (-38/+42)	+7 % (-4/+13)	+19 % (+10/+34)	+40 % (+20/+60)
	10	30 mm	+5 % (-54/+63)	+10 % (-3/+12)	+25 % (+12/+38)	+40 % (+20/+60)
	100	35 mm	+10 % (-70/+90)	+13 % (+4/+14)	+30 % (+15/+40)	+40 % (+30/+60)
Wind Gust	2	80 km/h	+0 % (-7/+8)	+3 % (+0/+4)	+3 % (-1/+4)	+2 % (+1/+4)
	10	96 km/h	-2 % (-17/+13)	+1.4 % (+0.1/+2.4)	+1.1 % (-1.8/+2.4)	+1.2 % (+0.6/+2.5)
	100	119 km/h	+2 % (-5/+10)	-0.4 % (-1.7/+0.2)	-0.5 % (-2/+0.2)	-0.4 % (-2/+0.3)
12h Snowfall	2	15 mm		-85 % (-94/-73)	-86 % (-96/-74)	-80 % (-100/-70)
	10	17.5 m		-69 % (-76/-58)	-68 % (-76/-59)	-69 % (-76/-58)
	100	22 mm		-6.0 % (-18/+13)	-0.3 % (-15/+20)	-4 % (-14/+30)
Storm surge + sea level rise	2	2.1 m		5 % (-0/+5)	10 % (-5/+15)	20 % (+10/+25)
	10	2.57 m		5 % (-5/+10)	5 % (+0/+10)	15 % (+5/+20)
	100	3.34 m		5 % (-10/+15)	0 % (-10/+10)	10 % (+0/+20)
Wave Height	2	6.36 m		-3 % (-8/+2)	-5 % (-11/+4)	-6 % (-9/-0.4)
	10	8.5 m		-5 % (-16/+6)	-7 % (-15/+8)	-10 % (-18/+8)
	100	12.08 m		-17 % (-19 /-15)	-25 % (-36/-15)	-23 % (-29/-16)

Not available

Significant increase P > 95%
 Not significant increase 50% < P < 95%
 Not significant changes P < 50%
 Not significant decrease 50% < P < 95%
 Significant decrease P > 95%

These values are practically identical for all return periods considered (2, 10 and 100 years), with the same median (Figure 14) and wide uncertainty ranges. Great variations are also expected for heat wave days, ranging the increase from +50% to up to +800% having a median of 280%, also by 2071-2100 period. As a result of this, hydrological drought is also expected to rise noticeably with high uncertainty, being the median an increase in 80% with an uncertainty interval from 25% to 90%.

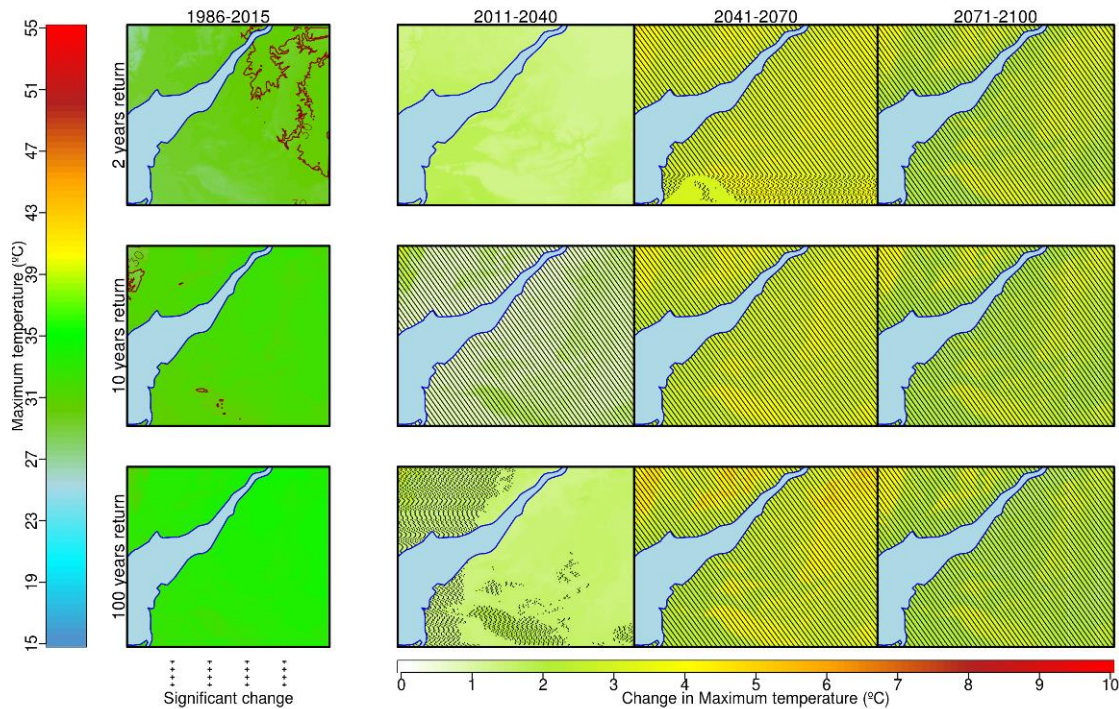


Figure 14. Multi-model median scenario of changes in extreme events of maximum temperature for the Bristol area, according to 2, 10 and 100-year return periods (rows) and for three future time periods (2011-2040, 2041-2070 and 2071-2100, second to fourth column) with respect to the reference period 1986-2015 (first column).

Extreme rainfall could increment about 30% at subdaily scale regarding most severe events (100-y return period) by the year 2100, with approximately a $\pm 15\%$ uncertainty level. Changes for the rest of period are also positive, around +10% for all return periods (Figure 15). Considering daily scale, changes are all positive, being especially significant for horizons 2041-2070 and 2071-2100, of up to $+40\% \pm 20\%$ by the year 2100 for the three represented return periods (2, 10 and 100 years). No remarkable change in extreme wind speed is expected, although significant, reaching a +3% increase throughout the whole century for 2 and 10-year return period, with a slight decrease (-0.5%) for the 100-year return period. Considering oceanic variables, little change in extreme wave height is observed, being in all case a decrease, with a peak change of -25% in expected maximum height in waves by 2041-2070 period for most extreme events (especially for 100-year return ones). However, storm surge is presumed to increase (considering too sea level rise) with a maximum of a +20% by 2071-2100 for most frequent events (2-year).

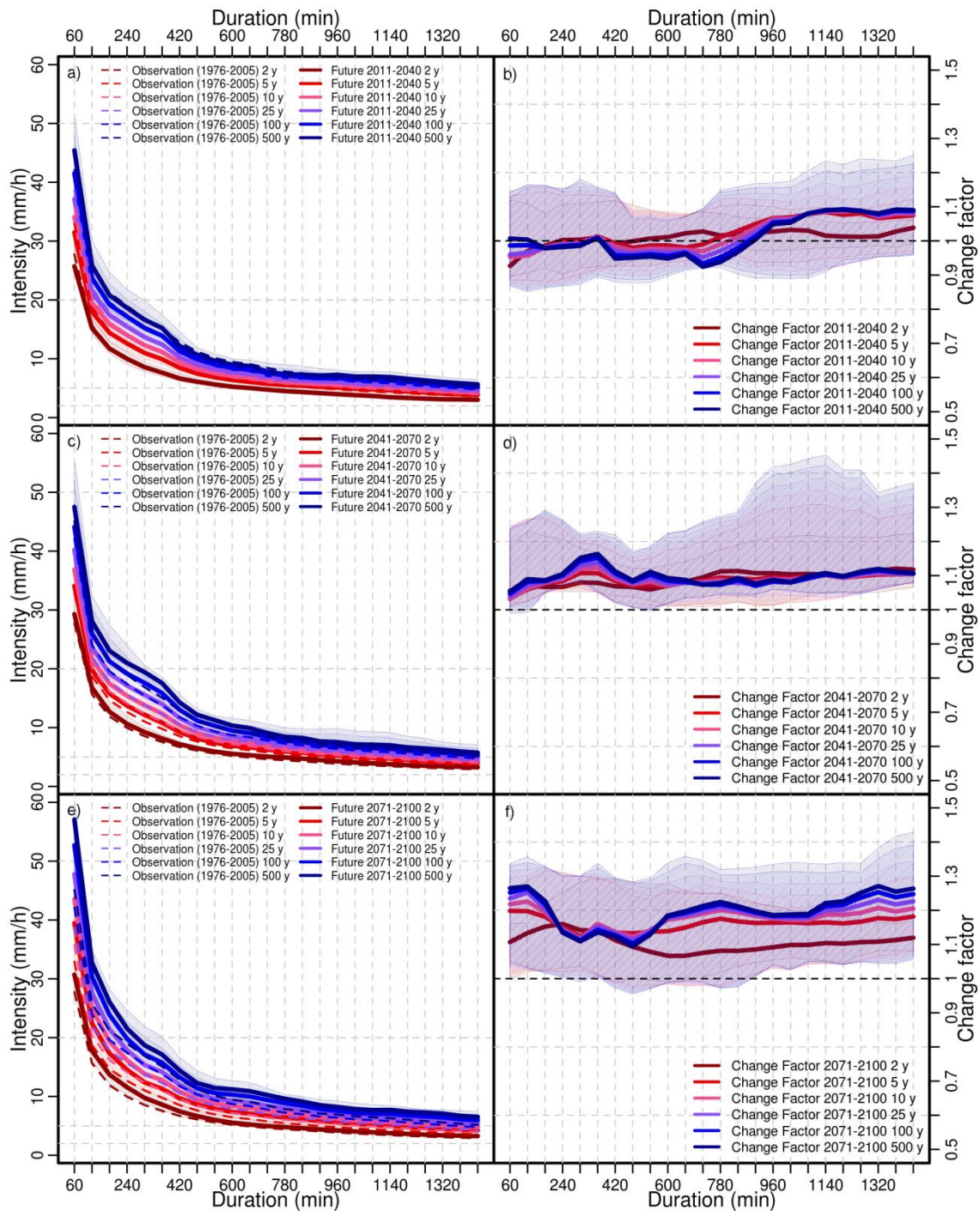


Figure 15. Projected IDF curves for the Bristol area (station No. 24615248) according to absolute values (left panels) and the change factor (right panels) for three future time periods: 2011-2040 (a, b), 2041-2070 (c, d) and 2071-2100 (e, f). Dashed coloured lines correspond to observations while thick ones represent simulations. Shaded areas represent uncertainty between quantiles 10th and 90th.

7. Conclusions

Near and long-term climate projections and seasonal predictions have been obtained for Barcelona, Lisbon and Bristol, including mean and extreme events by using several statistical downscaling methods applied to a set of CMIP5 climate models.

The used downscaling methods were verified using the ERA-Interim re-analysis as a reference for reproducing the past climate. In a similar way, application of these methods to global climate models was also validated according to several statistical measures. Both processes showed an adequate performance for all simulated climate variables, with negligible systematic errors. With respect to extreme events, systematic errors were small for most of the models and therefore corrected, especially in climate timescale. However, some nuances can stand out for the closest time horizons: seasonal and decadal simulations are adequate for extreme precipitation if teleconnection-based approach is used, while temperature is best simulated using drift-corrected dynamical outputs. Extreme wind speed is only adequately simulated for at climate timescale.

Regarding results for climate timescale, most important changes in the future climate are given by the temperature rise, with more than 2°C by 2100. The worst scenario (RCP8.5) projects a maximum warming up to 6°C in Barcelona and 5.5°C in Lisbon and Bristol. Rainfall could experience a significant increase between 5% and 40% in Bristol by 2100 under the RCP8.5 scenario. While for Lisbon, it would decrease down to -15% for the 2016-2035 period, and non-significant changes in annual rainfall are found for Barcelona, but with a high uncertainty. However, an increment of the potential evapotranspiration together with a possible decrease in snowfall between 50% and 100% in Barcelona and Bristol by 2100, would cause a greater water stress in Barcelona (up to +0.6 mm/day) and Bristol (up to +0.4 mm/day). Sea level rise is generally badly simulated even after the bias correction with just a few models passing most of the statistical test. Therefore, results of sea level projections should be taken with great caution, showing a rise of 50 cm in Lisbon and 60 cm in Bristol by 2100 under the RCP8.5. In Barcelona most probable scenario shows no significant changes in sea level but with high uncertainty.

Regarding extreme events results, extreme peak temperature values are expected to suffer a great rise, up to +3°C for Bristol and +5°C for Barcelona and Lisbon. Heat wave days will experience an increase greater than +100%, from 5 to 40 days per year in Barcelona, 20 in Bristol and 17 in Lisbon. Extreme precipitation will also increase in the three cities about +30%, Barcelona and Bristol in both daily and subdaily rainfall while Lisbon just for 1-hour (or shorter) events. Extreme snowfall could increase for 100y-return events in Barcelona up to 40%. Less extreme snowfall events (2-10 years return period) would suffer a great decrease in Bristol and Barcelona due to the temperature rise. On the other hand, pluviometric drought will not change significantly (i.e. SPI will not decrease), but hydrological drought will increment due to greater evapotranspiration (decrease in SPEI). Extreme wind gust could increase in Barcelona up to +10±3% the next two decades in all return periods, while storm surge combined with sea level rise is expected to increase in the three cities for 2y- and 10-return period by 2100. However, non-significant changes are projected for extreme wave heights in the RESCCUE cities.

References

- AEMET. 2016b. Olas de calor/frío en España desde 1975 Área de Climatología y Aplicaciones Operativas. Agencia Estatal de Meteorología (AEMET) open publications. Links:
http://www.aemet.es/documentos/es/noticias/2016/Olas_Calor_ActualizacionJun2016.pdf
http://www.aemet.es/documentos/es/noticias/2014/Olas_Frio_ActualizacionNov2014.pdf
- AMB, Altava-Ortiz V, Barrera-Escoda A, Amaro J, Cunillera J, Prohom M, Sairouni A. 2017. Escenaris climàtics futurs a l'àrea metropolitana de Barcelona. Direcció de Serveis Ambientals de l'Àrea Metropolitana de Barcelona (AMB).
- ARUP, Rockefeller Foundation. 2015. City Resilience and the City Resilience Framework: 100 Resilient Cities.
- Benestad RE. 2010. Downscaling precipitation extremes. Correction of analog models through PDF predictions. *Theoretical and Applied Climatology* 100: 1–21.
- Bentsen M, Bethke I, Debernard JB, Iversen T, Kirkevåg A, Seland Ø, Drange H, Roelandt C, Seierstad IA, Hoose C, Kristjánsson, JE. 2012. The Norwegian Earth System Model, NorESM1-M – Part 1: Description and basic evaluation. *Geoscientific Model Development Discussion* 5: 2843-2931. doi:10.5194/gmdd-5-2843-2012.
- Bi D, Dix M, Marsland S, O'Farrell S, Rashid H, Uotila P, Hirst A, Kowalczyk E., Golebiewski M., Sullivan A., Yan H., Hannah N, Franklin C, Sun Z., Vohralik P, Watterson I, Zhou X, Fiedler R, Collier M, Ma Y, Noonan J, Stevens L, Uhe P, Zhu H, Griffies S, Hill R, Harris C, Puri K. 2013. The ACCESS coupled model: description, control climate and evaluation. *Australian Meteorological and Oceanographic Journal*, 63: 41-64.
- Chylek P, Li J, Dubey MK, Wang M, Lesins G. 2001. Observed and model simulated 20th century Arctic temperature variability: Canadian Earth System Model CanESM2. *AtmosChemPhys Discuss* 11: 22893-22907, doi:10.5194/acpd-11-22893-2011.
- CML. 2016. Municipal Master Plan. URL: <http://www.cm-lisboa.pt/viver/urbanismo/planeamento-urbano/plano-diretor-municipal>.
- Collins M, Tett SFB, Cooper C. 2001. The internal climate variability of HadCM3, a version of the Hadley Centre coupled model without flux adjustments. *Climate Dynamics* 17: 61–81. doi:10.1007/s003820000094.
- CRU. 2017. Mediterranean Oscillation Index (MOI) data. Climate Research Unit. Link: <https://crudata.uea.ac.uk/cru/data/moi/> (Accessed on July 20 2017)
- Doblas-Reyes FJ, Andreu-Burillo I, Chikamoto Y, García-Serrano J, Guemas V, Kimoto M, Mochizuki T, Rodrigues LRL, van Oldenborgh GJ. 2013. Initialized near-term regional climate change prediction. *Natur Communications* 4:1715. DOI: 10.1038/ncomms2704.
- Dufresne J, Foujols M, Denvil S et al. 2013. *Climatic Dynamics* 40: 2123. doi: 10.1007/s00382-012-1636-1 Dunne JP, John JG, Adcroft AJ, Griffies SM, Hallberg RW, Shevliakova E, Stouffer RJ, Cooke W, Dunne KA, Harrison MJ, Krasting JP, Malyshev SL, Milly PCD, Phillipps PJ, Sentman LT, Samuels BL, Spelman MJ, Winton M, Wittenberg AT, Zadeh N. 2012. GFDL's ESM2 Global Coupled Climate–Carbon Earth System Models. Part I: Physical Formulation and Baseline Simulation Characteristics. *Journal of Climate* 25: 6646–6665. doi:10.1175/JCLI-D-11-00560.1.
- Gaetani M, Mohino E. 2013. Decadal Prediction of the Sahelian Precipitation in CMIP5 Simulations. *Journal of Climate* 26: 7708-2219.
- Hargreaves GH. 1994. Defining and using reference evapotranspiration. *Journal of Irrigation and Drainage Engineering* 120: 1132–1139.
- IPMA. 2016a. Climate Change in Portugal. Portal do Clima, Instituto Português do Mar e da Atmosfera (IPMA). URL:<http://portaldoclima.pt/en/>
- Iversen T, Bentsen M, Bethke I, Debernard JB, Kirkevåg A, Seland Ø, Drange H, Kristjánsson JE, Medhaug I, Sand M, Seierstad IA (2012) The Norwegian Earth System Model, NorESM1-M – Part 2: Climate response and scenario projections. *Geosci Model Dev Discuss* 5: 2933-2998. doi:10.5194/gmdd-5-2933-2012.
- JISAO. 2017. Joint Institute for the Study of Atmosphere and Ocean http://jisao.washington.edu/data_landing. (Accessed on July 20 2017)
- Kim HM, Webster PJ, Curry JA. 2012. Evaluation of short-term climate change prediction in multi-model CMIP5 decadal hindcasts. *Geophysical Research Letters* 39:L10701, doi:10.1029/2012GL051644

- Marsaglia G, Tsang WW, Wang J. 2003. Evaluating Kolmogorov's distribution. *J Stat Softw* 8:18
- Marsland SJ, Haak H, Jungclaus JH, Latif M, Roeske F. 2003. The Max-Planck-Institute global ocean/sea ice model with orthogonal curvilinear coordinates. *Ocean Modelling* 5: 91-127. doi: 10.1016/S1463-5003(02)00015-X.
- Martín-Vide J. 2004. Spatial distribution of a daily precipitation concentration index in peninsular Spain. *International Journal of Climatology* 24: 959–971.
- McKee TBN, Doesken J, Kleist J, 1993. The relationship of drought frequency and duration to time scales. In *Proceedings of the 8th Conference of Applied Climatology*, 17-22 January, Anaheim, CA. American Meteorological Society, Boston, MA. 179-184.
- Monjo R. 2016. Measure of rainfall time structure using the dimensionless n-index. *Climate Research*, 67: 71-86. doi: 10.3354/cr01359.
- Monjo R, Gaitán E, Pórtoles J, Ribalaygua J, Torres L. 2016. Changes in extreme precipitation over Spain using statistical downscaling of CMIP5 projections. *International Journal of Climatology* 36: 757-769. doi: 10.1002/joc.4380.
- Monjo R, Pórtoles J, Gaitán E, Ribalaygua J, Torres L. 2014. ¿Cambiará el régimen de precipitación extrema en España? IX Congreso Internacional AEC: Cambio climático y cambio global. Almería, 28 October. Link http://aeclim.org/wp-content/uploads/2016/02/0055_PU-SA-IX-2014-R_MONJO.pdf
- NOAA, 2017. Climate Indices. Enlace: <http://www.esrl.noaa.gov/psd/data/climateindices/list/> (Accessed on July 20, 2017)
- Pepler AS, Díaz LB, Prodhomme C, Doblas-Reyes FJ, Kumar A. 2015. The ability of a multi-model seasonal forecasting ensemble to forecast the frequency of warm, cold and wet extremes. *Weather and Climate Extremes* 9: 68–77, doi: 10.1016/j.wace.2015.06.005
- Redolat D. 2014. Simulación de los días de nieve a partir de predictores físicos y aplicación a proyecciones climáticas para alta montaña. Geography Degree Thesis. Complutense University of Madrid. Madrid, Spain.
- Redolat D, Monjo R, Lopez-Bustins JA, Martin-Vide J. 2017. Upper-Level Mediterranean Oscillation index and seasonal variability of rainfall and temperature. *Theoretical and Applied Climatology* (in review).
- Ribalaygua J, Torres L, Pórtoles J, Monjo R, Gaitán E, Pino MR. 2013. Description and validation of a two-step analogue/regression downscaling method. *Theoretical and Applied Climatology*, 114: 253-269. doi:10.1007/s00704-013-0836-x.
- SMC. 2015. Balanç d'una de les onades de calor més intenses de les últimes dècades. Link: http://premsa.gencat.cat/pres_fsvp/AppJava/notapremsavw/286294/ca/balanc-duna-onades-calor-intenses-decades.do.
- Taylor AH. 2011. *The Dance of Air and Sea: How Oceans, Weather and Life Link Together*. Oxford University Press, 288 pp.
- Thorntwaite CW. 1948. An approach toward a rational classification of climate. *Geographical Review* 38: 55-94, doi:10.2307/210739
- UB. 2017. University of Barcelona. <http://www.ub.edu/gc/2016/06/08/wemo/>. (Accessed on July 20 2017).
- Venables WN, Ripley BD. 2002. *Modern Applied Statistics with S*. New York: Springer (4th ed).
- Voldoire A, Sanchez-Gomez E, Salas y Méliá D, Decharme B, Cassou C, Sénési S, Valcke S, Beau I, Alias A, Chevallier M, Déqué M, Deshayes J, Douville H, Fernandez E, Madec G, Maiconnave E, Moine M-P, Planton S, Saint-Martin D, Szopa S, Tyteca S, Alkama R, Belamari S, Braun A, Coquart L, and Chauvin F. 2013. The CNRM-CM5.1 global climate model: description and basic evaluation, *Climate Dynamics* 40: 2091-2121, doi: 10.1007/s00382-011-1259-y.
- Watanabe S, Hajima T, Sudo K, Nagashima T, Takemura T, Okajima H, Nozawa T, Kawase H, Abe M, Yokohata T, Ise T, Sato H, Kato E, Takata K, Emori S, and Kawamiya M. 2011: MIROC-ESM 2010: model description and basic results of CMIP5-20c3m experiments. *Geoscientific Model Development* 4: 845-872. doi:10.5194/gmd-4-845-2011.
- WMO. 2001. WCDMP-47: Report on the activities of the working group on climate change detection and related rapporteurs, 1998-2001. WMO/TD-No.1071.
- WMO. 2017. Guidelines on the Definition and Monitoring of Extreme Weather and Climate Events, draft version, WMO-No.1204. Link: https://library.wmo.int/opac/doc_num.php?explnum_id=4213. ISBN: 978-92-63-11204-0.

- Xiao-Ge X, Tong-Wen W, Jie Z. 2013. Introduction of CMIP5 Experiments Carried out with the Climate System Models of Beijing Climate Center. *Advances in Climate Change Research*4: 41-49. doi: 10.3724/SP.J.1248.2013.041.
- Yukimoto S, Yoshimura H, Hosaka M, Sakami T, Tsujino H, Hirabara M, Tanaka TY, Deushi M, Obata A, Nakano H, Adachi Y, Shindo E, Yabu S, Ose T and Kitoh A. 2011. Meteorological Research Institute-Earth System Model Version 1 (MRI-ESM1) - Model Description. Technical Report of MRI, No. 64, 83 pp.
- Zhang X, Alexander L, Hegerl GC, Jones P, Tank AK, Peterson T, Trewin B, Zwiers F. 2011. Indices for monitoring changes in extremes based on daily temperature and precipitation data. *WIREs Climate Change*, doi: 10.1002/wcc.147. Link: https://www.geos.ed.ac.uk/homes/ghegerl/WIRES_index.pdf
- Zorita E, Hughes J, Lettenmaier D, Storch Hv. 1993. Stochastic downscaling of regional circulation patterns for climate model diagnosis and estimation of local precipitation. Max Planck Institute for Meteorology Technical Report 109.